Strengthening of Wooden Cross arms in 230 kV Transmission Structures using Glass Fibre Reinforced Polymer (GFRP) Wrap

by

Arash Shahi

A thesis
presented to the University of Waterloo
in fulfillment of the
thesis requirement for the degree of
Master of Applied Science
in
Civil Engineering

Waterloo, Ontario, Canada, 2008

AUTHOR'S DECLARATION

I hereby declare that I am the sole author of this thesis. This is a true copy of the thesis, including any required final revisions, as accepted by my examiners.

I understand that my thesis may be made electronically available to the public.

Abstract

There are approximately 6000 Gulfport-type wood structures used to support 1600 km of 230 kV electrical transmission lines in Ontario. An unexpected structural failure caused by wood deterioration has been recognized as a major risk to the safety of these transmission lines. Since the reliability of the electricity transmission and distribution lines is extremely important to the electrical industry and other users of electricity, failure of these structures can result in devastating incidents. Due to the remote location of the transmission network and the requirement to keep the power lines in continuous service, replacement of the Gulfport structures has proved to be very difficult and expensive. This research program investigated the use of Glass Fibre Reinforced Polymer (GFRP) wrap as a light weight and durable strengthening system that can be applied to the existing structures without any interruptions in the functionality of the transmission lines.

A total of three control specimens and three strengthened samples were tested in Phase I of the experimental program, which was designed as a feasibility study. It was concluded that the average strength of strengthened samples was 42% higher than the average strength of the control samples, and was greater than the end of life (EOL) threshold of 30 MPa for the cross arms. Therefore, the proposed strengthening system was concluded to be an effective solution for strengthening the deteriorated cross arms of the Gulfport structures. Taguchi methods and Analysis of Variation (ANOVA) were employed in Phase II to optimize the proposed strengthening system. The optimal configuration was determined to be the application of the filler material, non-sanded surface, and the shorter width of wrap (width of 0.6 m). The mean strength of the optimal configuration was estimated to be 52 MPa with a 95% confidence interval of: 38.7 MPa < True Mean < 65.3 MPa. Phase III confirmed the estimated mean and the confidence interval for the optimal configuration in Phase II. The strengthening system changed the failure mode from combined shear-flexure failure to pure flexure and resulted in more consistent strength and stiffness values. The strain values of the GFRP wrap showed that a single layer of wrap was sufficient for the confinement purposes.

Acknowledgements

I would like to express my sincerest appreciation and gratitude to my supervisors, Prof. Jeffery S. West and Prof. Mahesh Pandey for their guidance, motivation, unconditional help and support, and for always believing in me during the past two years. I would also like to thank Prof. Ajay Batish for his advice and guidance throughout the experimental design aspect of this research.

I would like to thank the readers of my thesis, Prof. Scott Walbridge and Prof. Carl T. Haas, for their insightful comments and suggestions.

I wish to thank Doug Hirst for his help and support in the lab. I would also like to thank the other technicians that helped me to get through this project: Ken Bowman, Terry Ridgway, and Richard Morrison.

I would like to express my special thanks to my friend and officemate Dr. Han Tea Choi for putting up with me for the last two years and for providing brilliant solutions to every complicated problem. Special thanks goes out to my Undergraduate Research Assistants Kyla Tan and Robert Lepage and my Co-op student Taraneh Shahi for providing extra set of hands, great ideas, and hard work which helped me to get through my research program in difficult times.

Last but not least I would like to thank my parents Sussan and Davood for their unconditional love and support, my sister Sheida for always being there for me, and my wife Taraneh for everything.

To my parents Sussan and Davood,
my lovely sister Sheida,
and my beautiful wife Taraneh

Table of Contents

List of Figures

List of Tables

1 Introduction

1.1 General

Electricity transmission lines provide a connection between high voltage generation to local industrial and residential users. Steel transmission towers are the most common structures for carrying high voltage lines particularly in urban areas where the impact of a power failure could be catastrophic. However, in remote areas where the transmission security class is lower, wooden structures are used to support the transmission lines up to a maximum of 230 kV. Gulfport-type wood structures, or a minor variation of them, have been used as the primary means of transmission and distribution of electricity in the remote areas in North America (McCarthy 2005). The majority of these structures were constructed 30-40 years ago, and some have experienced severe deterioration.

Since the reliability of the electricity transmission and distribution lines is extremely important to the electrical industry and other users of electricity, failure of these structures can result in devastating incidents such as the blackout on August 14th, 2003 in Canada (Natural Resources Canada 2003). Therefore such failures have to be prevented by ensuring that the condition of these structures meets the design requirements despite the level of deterioration that may have occurred.

There are approximately 6000 Gulfport-type wood structures used to support 1600 km of 230 kV electrical transmission lines in Ontario (McCarthy 2005). An unexpected structural failure caused by wood deterioration has been recognized as a major risk to the safety of these transmission lines. Figure 1 shows a schematic of a Gulfport structure with approximate dimensions of the members. Gulfport structures are discussed in detail in the following sections of this thesis. Previous research at the University of Waterloo has identified the most critical element of the Gulfport structures to be the cross-arms, particularly between the main poles and brace supports, as indicated in Figure 1 (McCarthy 2005).

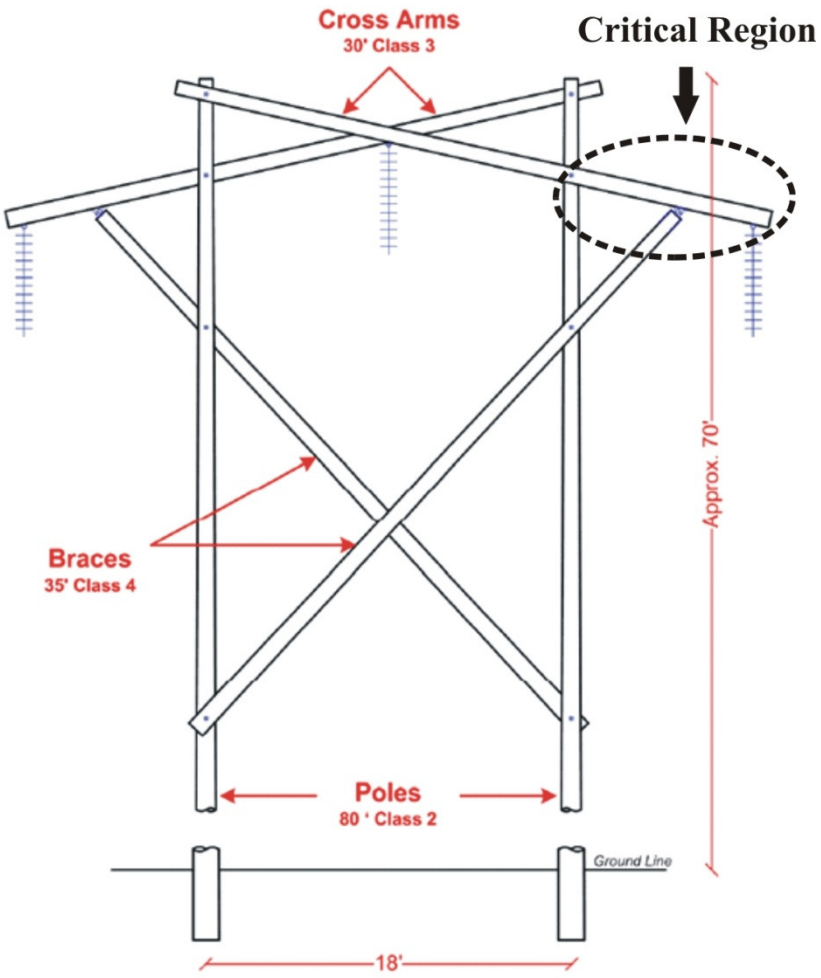

Figure 1: Gulfport Structure and the Critical Region (McCarthy 2005)

Due to the remote location of the transmission network and the requirement to keep the power lines in continuous service, replacement of the Gulfport structures has proved to be very difficult and expensive. As a result, alternatives for in-service rehabilitation and strengthening must be explored. Fibre Reinforced Polymer (FRP) materials have been used increasingly as a structural repair system in the last decade due to the many advantages that they have over the traditional steel strengthening systems. This research program investigated the use of Glass Fibre Reinforced Polymer (GFRP) wrap as a light weight and durable

strengthening system that can be applied to the existing structures without any interruption to the functionality of the transmission lines.

1.2 Objectives

The overall objective of this research program was to establish an efficient and effective strengthening system for in-situ rehabilitation of Gulfport cross-arms using Glass Fibre Reinforced Polymer (GFRP) wrap. This main objective was achieved by:

- Conducting a feasibility study on the critical section of the Gulfport cross-arms to ensure that the required strength increase could be achieved using the proposed strengthening system;
- Developing a statistically designed parameter optimization experimental program to determine the most critical factors involved in the strengthening system and to obtain the optimal configuration of those factors to achieve the maximum strength, and;
- Using statistical tools to estimate the mean and a confidence interval for the proposed optimal configuration of the strengthening system, and by designing a separate experimental program to confirm the analytical estimates of the mean and the confidence interval.

1.3 Thesis Arrangement

In Chapter 2, a general structural analysis of the Gulfport structures is presented along with a review of the existing literature and background information related to strengthening of timber elements with Fibre Reinforced Polymer (FRP) materials. Since the published literature on strengthening of timber elements with GFRP material was very limited, the relevant literature focussing on concrete applications are also presented and potential similarities to timber applications are noted.

Chapter 3 describes the three separate phases of the experimental program. Taguchi methods and Analysis of Variation (ANOVA) techniques that were used to develop the Phase II of the experimental program are explained in detail in this chapter. The test setup and equipment, the variables investigated, the sample preparations, data acquisition system, and the testing procedures for material testing as well as three-point bending tests are also presented in this chapter.

In Chapter 4, the results from the three phases of the experimental program are presented, analyzed, and discussed. The implementation of the ANOVA analysis is also demonstrated and statistical analysis of the results is presented including the concepts and equations required to perform the ANOVA analysis. The results from small scale testing are also presented and analyzed in this chapter.

Chapter 5 described the performance of the strengthening system with respect to the structural requirements of the Gulfport structures. The failure mechanism of the strengthened specimens is discussed in this chapter along with the analysis of the strain data. Local failures caused by the high loads that were experienced by the strengthened specimens are also discussed in this chapter.

The conclusions of all aspects of this research program are summarized in Chapter 6. A number of recommendations for improving the proposed strengthening system as well as recommendations for future research in this area are also presented in this chapter.

2 Gulfport Analysis and Literature Review

2.1 Gulfport Analysis

The loading that is imposed on Gulfport structures consists of the dead weight of the three supported conductors and insulators, snow load, ice load, and wind load. The self weight of the structure is insignificant in comparison to the imposed loads. The controlling design factors for transmission structures in Ontario include: wind loads, ice and snow accumulation on the cables, and the span between the structures (McCarthy 2005). Figure 2 illustrates the horizontal and vertical spans that were used for the design of Gulfport structures. The horizontal span is the distance between the mid-spans of the adjacent spans and is used for wind loads, while the vertical span is the distance between the lowest points on the sag curve of the two adjacent spans and is used for the vertical loads. A typical horizontal span for Gulfport structures in Ontario is approximately 300 m (McCarthy 2005).

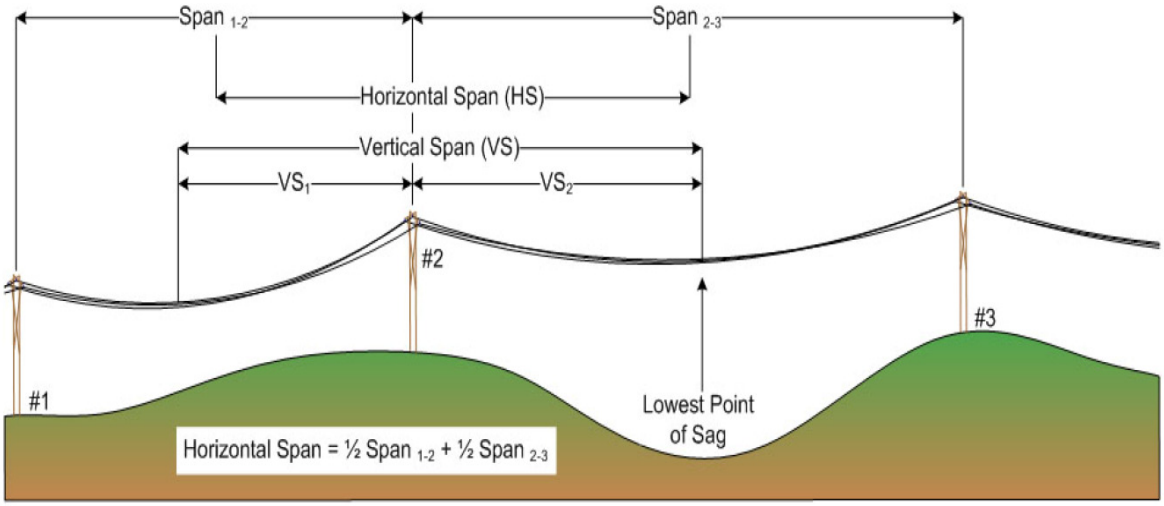

Figure 2: Gulfport Structure Spans (McCarthy 2005)

McCarthy (2005) conducted an extensive condition assessment study on Gulfport structures at University of Waterloo. That research used the design guidelines from the Canadian Standards Association (CSA C22.3 No. 1-01) and the wind and snow loads for Northern Ontario to calculate the design loads of the Gulfport structure for the Northern Ontario region. The resulting loading on the structure, including load factors for dead loads, ice loads, and wind loads are shown in Figure 3.

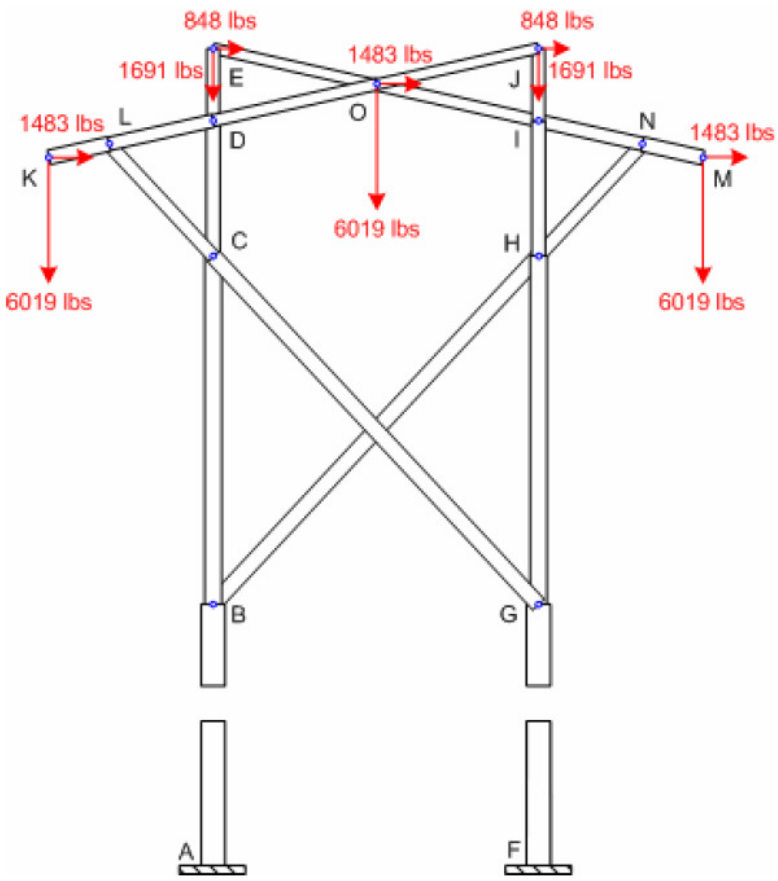

Figure 3: Gulfport Factored Design Loads (McCarthy 2005)

The average diameter of the different elements of the Gulfport structure, determined through an extensive survey by Ontario Hydro is presented in Table 1 (McCarthy 2005).

Table 1: Typical Gulfport Member Diameters

Member	Specification	Section	Average Diameter (cm)
Pole	Western Red Cedar, 80 ft.	AB, FG	38.1
		BC, GH	27.8
		CD, HI	23.2
		DE, IJ	21.3
Cross Arm	Jack Pine, 30 ft.	KL, MN	27.0
		LD, NI	25.2
		DO, IO	22.2
		OJ, OE	18.5
Brace	Jack Pine, 35 ft.	BH, GC	24.0
		HN, CL	18.3

The bending moment diagram of the Gulfport structure based on the design loads of this structure in Northern Ontario is presented in Figure 4. The maximum bending moment in the cross arms at the critical section, identified earlier in Chapter 1, is 23.0 k-ft, which corresponds to 31.2 kN-m.

The material properties published by CSA-O15-90 were used for the purposes of the evaluation of Jack Pine species used for the cross arms of the Gulfport structure: Modulus of Elasticity of 8.4 GPa and Modulus of Rupture of 45 MPa. The Canadian and American standards, CSA C22.3 No.1-01 and National Electrical Safety Code C2-1993, define the end of life (EOL) of a cross arm as the point when the pole has deteriorated to two thirds of its original strength (McCarthy 2005). Therefore, the EOL for Gulfport cross arms in terms of the Modulus of Rupture is 30 MPa. Cross arms having tested or assumed modulus of rupture less than the EOL value would be deemed inadequate and had to be replaced.

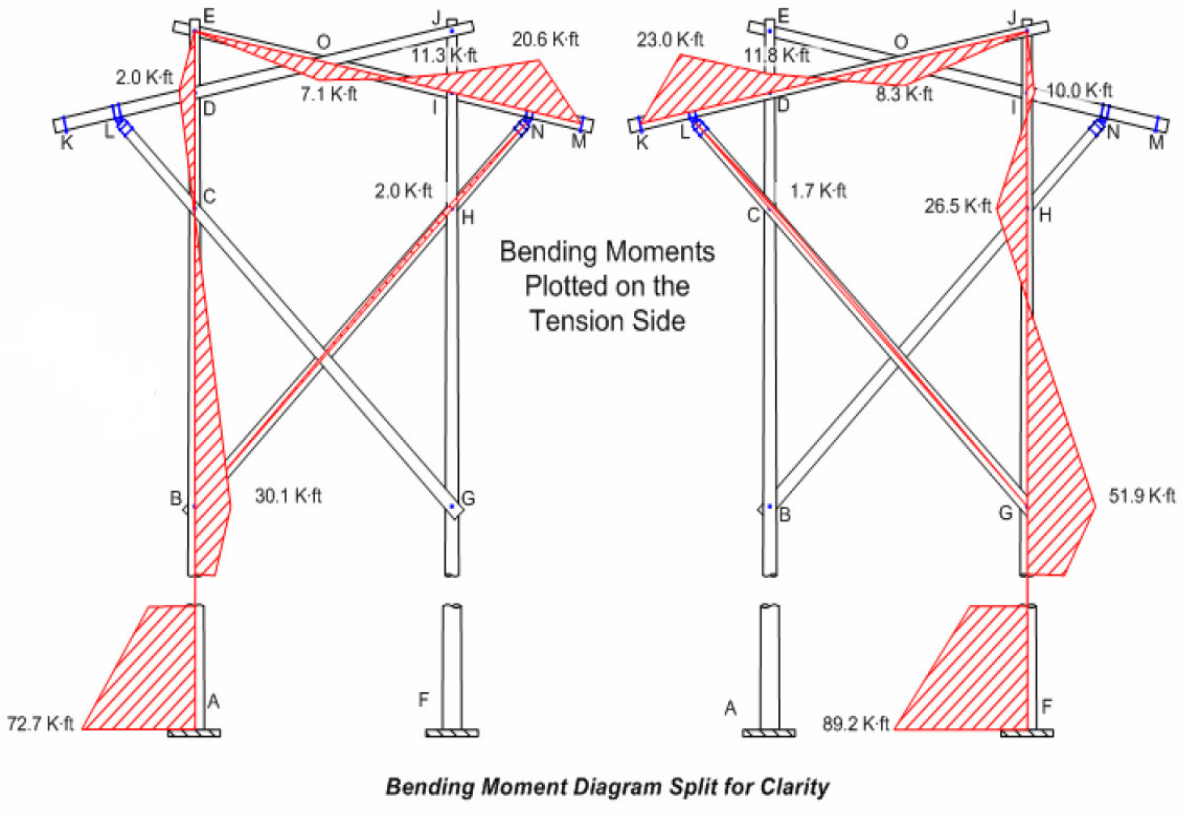

Figure 4: Factored Bending Moment Diagram for Design Loads (McCarthy 2005)

2.2 Literature Review

Fibre reinforced polymer (FRP) materials have gained considerable popularity as a reinforcement alternative to steel in the last decade. The corrosion resistance of FRP materials is one of the most important advantages of this type of reinforcement in comparison to steel. This advantage has motivated extensive research in the area of strengthening of concrete structures using FRP materials (Nanni and Norris 1995). An extensive review of the existing literature revealed that the effect of FRP materials have not been investigated in all areas equally. For example, although extensive literature background is available for reinforcing concrete beams, limited research has specifically addressed FRP strengthening of concrete poles (Soudki and Chahrour 2006). Also, research on FRP strengthening of wood structures is comparatively limited, and has primarily focused on flexural strengthening with

FRP strips (Gilbert et al. 2003). Notably, there is little or no research on the strengthening of deteriorated wood elements, nor for wood members with circular cross sections such as the Gulfport cross-arms, where FRP wrapping and flexural strengthening may be employed.

The extensive research background has motivated the field application of FRP reinforcement for concrete structures. However, in order to implement FRP reinforcement on deteriorated wooden circular members, more research and greater understanding of the behaviour of FRP strengthened wood poles are required. Due to the lack of literature on this topic, the performance of FRP materials on concrete structures was investigated and potential relationships to timber structures were noted. A number of these relationships were tested and verified as part of the experimental program of this research program.

2.2.1 FRP Strengthening of Concrete Structures

FRP reinforcement can be used both in the shape of traditional steel reinforcement bars and also as confinement wraps around the structure. The confinement method for FRP reinforcement is particularly advantageous over steel confining jackets due to the larger contact area, flexibility in construction and design, and greater ease of installation (Nanni and Norris 1995). Many researchers have verified the effectiveness of the FRP wraps in increasing the strength of reinforced concrete elements and have reported strength gains of up to 100% in some cases (Au and Buyukozturk 2005). The confinement wraps may increase both the flexural and compressive strengths of the member. However, the extent of strength gain of each reinforced specimen is dependent upon many variables, such as the fibre orientation, number of layers of wrap, and the bond strength between FRP wrap and concrete.

A recent study investigated the strengthening of deteriorated concrete light poles using FRP sheets (Soudki and Chahrour 2006). In this study, the effect of bidirectional versus unidirectional wraps was examined. Furthermore, a comparison between glass and carbon sheets was conducted. The maximum experimental capacity was reached by using

bidirectional E-glass FRP sheets. It was concluded that the bidirectional flexure sheets had greater effect on restoring the flexural strength of the damaged poles than the lateral unidirectional confining sheets. It was also concluded that poles reinforced with GFRP wraps produced higher strengths and greater flexibilities than those reinforced with CFRP wraps, both in bidirectional and unidirectional configurations. All of the poles that were reinforced in this study exhibited a change in the failure mode from compressive flexural to tensile flexural which is more ductile and more favourable (Chahrour and Soudki 2006). Other researchers also concluded that external confinement of concrete using FRP material can significantly increase both strength and ductility of concrete (Mirmiran and Shahawy 1997). The latter study also concluded that confinement of concrete by FRP material results in large energy absorption capacity.

Au and Buyukozturk (2005) performed a study on the effect of fibre orientation on FRP-confined concrete. In this study, the samples were tested in axial compression. They concluded that when loaded in axial compression, the best wrapping strategy was wrapping one underlying layer at 45 degrees with unidirectional lateral wrap on top of that. Interestingly, bidirectional wrap was ranked lowest in this study. They also concluded that under axial compression, the unidirectional wrap led to brittle failures, while helical wrap failed in a ductile manner. The contrasting results in these studies suggest that the loading mechanism dictates the optimal wrapping strategy.

Bonacci et al. (2001) investigated the effect of prestressing of the FRP wraps on the strength of the corrosion-damaged concrete columns. FRP wraps were prestressed by applying a 25mm think layer of expansive grout on the surface of concrete that expanded approximately 2.5% after application and prestressed the FRP wraps (Bonacci et al. 2001). Their research concluded that prestressing reduces the available deformation capacity of the jacket as well as keeping the moisture inside the core and thus accelerating the corrosion process. However, some positive conclusions were also made in their study. They concluded that the strength of the column had a strong positive correlation with number of layers of wrap (Bonacci et al.

2001). This conclusion suggested that by conducting a cost effectiveness analysis, the optimal number of wraps can be determined for a given FRP-wrap strengthening system.

It is important to note that only the research studies that were related to the research program of this thesis have been presented in this section. Presenting all of the published literature on the strengthening of concrete structures using FRP material was beyond the scope of this thesis. Several state of the art reports are available on strengthening concrete structures using FRP materials including ACI 440R-07 (ACI Committee 440 2007).

The failure mechanisms of deteriorated concrete poles are inherently different from those of deteriorated wood elements due to the nature of wood and the differences in type and level of deterioration that concrete and wood normally experience. Therefore, prior to any conclusions being made from previous research on concrete applications, the effect of the increasing number of layers of GFRP wrap as well as the effect of the orientation of the wrap has to be experimentally confirmed on circular deteriorated wood elements. Testing these parameters was beyond the scope of this research program, but they are presented as recommendations for future research projects in this field.

2.2.2 FRP Strengthening of Timber Structures

The literature and the extent of research on wood members were very limited in comparison to concrete structures at the time this research was conducted. There were very few publications on reinforcing circular flexural elements and no literature on deteriorated circular wood members reinforced with FRP material. The lack of literature in this area motivated this research. However, there were a number of previous research projects that were closely related to one or more aspects of this research, which are presented in this section.

FRP materials are highly advantageous in comparison to steel reinforcement for wood applications. FRP materials bond to timber very easily, and have a low density with high

strength and stiffness. Most importantly, and unlike steel, they are more compatible to timber in terms of strains at failure, which allows the full utilization of the timber strength (Gilbert et al. 2003). Due to the above disadvantages of steel for wood applications, using steel based strengthening system was not investigated in the published literature, and it was also not considered in the research program of this thesis. Based on material stiffness, carbon fibre reinforced polymer is more compatible with concrete, and glass fibre reinforced polymer is more compatible with wood. Therefore, the current research study has utilized the GFRP material for the purposes of reinforcing wood members.

Gentile et al. (2002) conducted a research study on 30 year old timber beams taken out of service from a bridge. They reinforced the members using GFRP bars bonded into grooves cut into the tension side of the beams referred to as near surface mounted bars. Gentile et al. concluded that using near surface GFRP bars enhanced the bending strength of wood structures by overcoming the negative effects of local defects in the wood. They also concluded that GFRP reinforcement prevented crack openings and confined local rupture of the wood, which resulted in a 64% increase in ultimate tensile strain of the strengthened beams (Gentile et al. 2002). Their study was particularly significant as they verified their findings by in-situ application of the reinforcement under full traffic loads over the bridge. Gentile et al. observed a failure mode change from brittle tensile failure in the unreinforced members to a ductile compressive failure in the reinforced specimens.

Figure 5 illustrates a comparison between a brittle tensile failure and a ductile compressive failure in timber beams, tested by Gilbert et al. (2003). They also observed a failure mode change from tension failure to compressive failure by reinforcing timber beams by FRP materials.

Borri et al. (2005) investigated the possibility of reinforcing old wood beams with FRP material. They compared the use of FRP rods and FRP sheets for reinforcing the flexural beams on the tension side of the member. The use of FRP sheets was found to increase the

flexural capacity of the beams by up to 60% compared to unreinforced specimens. Borri et al. concluded that since wood members are relatively flexible with large deflections at failure, using FRP rods was not very effective as they reduced the maximum deflection of the member at failure. FRP wraps, however, increased both the deflection limit and flexural capacity of the member, resulting in a ductile failure mode (Borri et al. 2005).

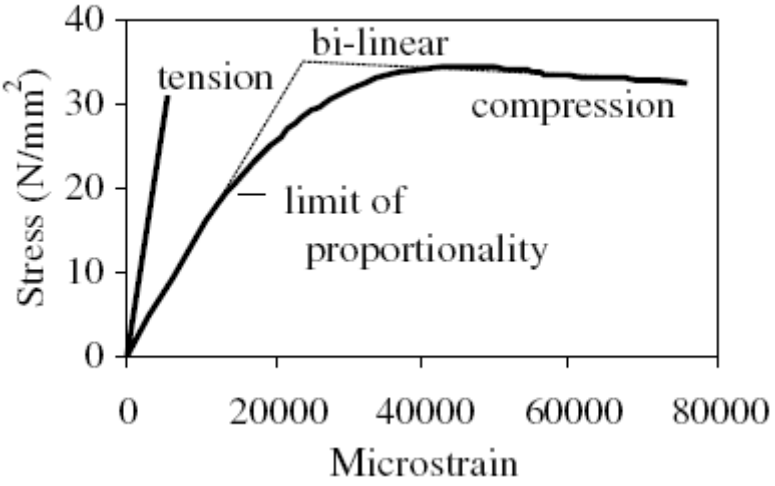

Figure 5: Typical Stress-strain Behaviour of Timber Members (Gilbert et al. 2003)

The FRP wraps, both in reinforcing concrete and timber members, are usually oriented so as to develop their tensile resistance in the direction transverse to the beam axis. If the wrap is properly secured and anchored, it can contain the delamination of the member, and can generate very large confining stresses on the core of the member (Bonacci et al. 2001).

Davalos et al. (1999) conducted a feasibility study using GFRP wraps for strengthening wood railroad crossties. Crossties removed from service were wrapped with a relatively thin layer (1.78 mm) of GFRP wrap and tested in bending to failure. As with other research studies on reinforcing flexural members with FRP materials, the failure mode for the strengthened crossties was a ductile compression failure without fracture of the FRP material, as opposed to tension failure and fracture through the cross section of the unreinforced control

specimens. The results demonstrated strength increases of about 29% for initially dry strengthened members and up to 70% for originally wet strengthened members. Therefore, the reinforcement affected the weaker specimens to a greater extent (Davalos et al. 1999). This study also concluded that the effect of moisture on reinforced specimens, which was considered as a weakening mechanism, was 47% less than its effect on unreinforced specimens. Therefore, the FRP strengthened members demonstrated a greater consistency and their strength was less dependent on original condition of the member.

In addition to the strength gain associated with the reinforcement, FRP strengthened timber elements also behave in a much more consistent manner than unreinforced members (Ahmed and Lyons 2005). Since wood is a natural material, any wood structure has high variability in terms of stiffness and strength, mainly due to the presence of knots, branches, and variable density of the material. Based on the observations by Davalos et al. and Ahmed and Lyons, it was hypothesized that the strength of the deteriorated circular members strengthened with GFRP wrap may not be strongly influenced by the extent of their original deterioration. This would make the strengthening strategy less reliant on a condition assessment of the existing structures, which would be very beneficial to the application of this strengthening system to in-service structures. If the weak members experience a higher strength gain percentage relative to the stronger samples, the reinforced specimens would all fail at approximately the same maximum load. This hypothesis was critical to the results of this research as it would demonstrate a high level of consistency and therefore a high level of reliability for the proposed strengthening system.

2.2.3 FRP Jacketing Shells

Limited research has focused on using prefabricated FRP shells instead of field lay up of FRP wraps on structures. Prefabricated shells would potentially be very suitable and practical for the purposes of remote structures that are not easily accessible and need to be strengthened in place. However, experiments with FRP shell have revealed some negative consequences which suggest that this technology was not yet well developed at the time these

studies were conducted. The implementation of FRP shells technology was beyond the scope of this research program, but one study is presented to highlight the possible option for future research in this area.

Nanni and Norris explored the option of FRP shells and compared their effectiveness to FRP wraps. Their study concluded that while FRP wraps increased both the strength and ductility of the structures, prefabricated shells had a minimal, and often no positive effect, over the unreinforced specimens. Experiments on circular sections revealed that the unreinforced specimens outperformed those confined by prefabricated FRP shells (Nanni and Norris 1995). This unexpected result was due to the disintegration of the grout placed between the shell and the concrete and due to the low ductility of the shell.

Due to the lower material stiffness of wood in comparison to concrete, wood poles will experience larger deflections than concrete poles and therefore the problems that were associated with FRP shells with concrete poles would be magnified. Therefore it was concluded that this option was not practical in its current form for the purposes of reinforcing deteriorated timber poles in Gulfport structures.

2.2.4 Bond Strength

A major concern with regards to reinforcing deteriorated wood members with GFRP wrap was the bond strength between the reinforcement and the deteriorated surface. Although there was no literature on bonding GFRP wrap to deteriorated wood, the bond quality of FRP wrap on deteriorated concrete was previously studied (Alampalli 2006). A study by Alampalli (2006) investigated the effect of surface condition of deteriorated concrete poles on the bond quality of FRP wraps and concluded that the quality of the bond was irrespective of the level of surface deterioration.

Lyons and Ahmad investigated the different factors that were expected to affect the bond between FRP composites and wood, including moisture content of the wood, magnitude and

direction of applied loads, level of deterioration of the wood surface, design life, and the operating environment (Ahmed and Lyons 2005). Adhesive characteristics and use of primers were also investigated as part of this study. Lyons and Ahmad concluded that FRP wraps bond better to dry wood and rough surfaces, although the effect of rough surface was deemed insignificant (Ahmed and Lyons 2005). The significance of this finding was that timber poles may not need to be sanded in order to improve the bond, which would improve the practicality of on-site remediation. They also reported a significant increase in the strength of all FRP wrapped wood structures compared to unreinforced structures.

2.3 Summary

The advantages of the FRP material over the steel reinforcement have motivated extensive research on the application of FRP materials on concrete. These advantages include material characteristics such as corrosion-resistivity, light weight, durability, and high strength to weight ratio as well as ease of installation and ease of use in a variety of applications. Many researchers have investigated the use of FRP rods, plates, and sheets for reinforcement in new concrete construction and strengthening of existing structures. However, the research on the application of FRP material on timber elements is very limited, with no published literature on strengthening of deteriorated circular elements, such as Gulfport structures.

Due to the inherent differences between concrete and timber applications, the conclusions that were made in studies based on concrete applications cannot be directly applied to timber applications. Therefore the factors that were deemed significant to the application and effectiveness of the proposed strengthening system on Gulfport structures were identified using the published literature on concrete applications and were then built into the testing program of this thesis. The factors affecting bond such as surface deterioration, sanding, and use of filler material were tested as part of the experimental program. Although the application of bidirectional wrap was beyond the scope of this research, the effect of varying the width of the applied wrap was also investigated. The industry acceptance of FRP material

on concrete applications is much greater than for timber applications, mainly due to the lack of knowledge and expertise in strengthening timber structures with FRP material. The lack of research and literature in this category has motivated this research program, which aims at identifying new applications for FRP material in the timber industry.

3 EXPERIMENTAL PROGRAM

3.1 Introduction

The experimental program of this research was conducted in three separate phases, with each subsequent phase relying on the results of the previous phase. Phase I was conducted to investigate the feasibility of the proposed strengthening system on Gulfport cross-arms. Phase II was conducted as the parameter optimization process for the strengthening system proposed in Phase I. In order to achieve the most efficient testing program, Taguchi Method and Analysis of Variation (ANOVA) were used to design the experimental program in Phase II. These statistical tools are explained in detail in this chapter. Phase III involved the confirmation testing of the optimal configuration obtained from Phase II of the experimental program. The confirmation testing is an essential aspect of the Taguchi Design.

The test setups for all three phases were the same and are presented in this chapter, prior to the discussion of the separate phases of the testing program. Material testing was performed on wood samples from the cross-arms as well. These included Shear-Parallel-to-Grain, Compression-Parallel-to-Grain and Moisture Content tests, which are also presented in this chapter.

3.2 Test Setup and Instrumentation

Previous research at the University of Waterloo had identified the most critical region of the Gulfport structures to be the cross-arms, particularly between the main pole and the brace supports (McCarthy 2005), as illustrated previously in Figure 1. The cross-arm elements are approximately 10 meters long. Based on the previous research, it was decided to test only the critical region shown in Figure 1. Therefore, the testing program was based on 3.2 m specimens that were cut from the cross-arm elements to represent the critical region of the

cross-arms. The specimens that were used in this testing program were removed from actual Gulfport structures and are considered to be a true representation of the cross-arms in service.

The cross-arm specimens were tested in flexure in three-point bending to failure. The details of the test setup were chosen to represent the real loading and support configuration of in-service cross-arm members. In addition, original connection and support hardware for cross-arm members were used where possible. Figure 6 presents a schematic of the test configuration that was used to represent the critical region of the cross-arms.

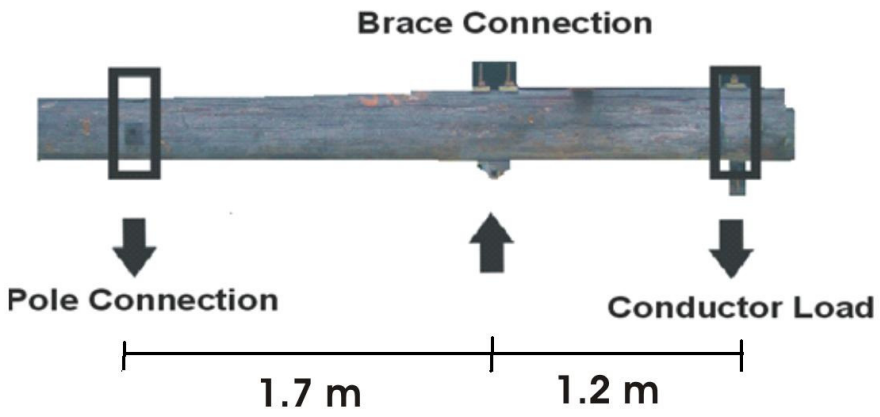

Figure 6: Schematic Test Configuration – Critical Region of Cross-arm

The specimens were tested in the structures laboratory at the University of Waterloo using the test setup shown in Figure 6. Loading was applied using a servo-controlled 35 kip actuator. Four deflection readings were taken under the specimen using displacement potentiometers or Linear Variable Differential Transformers (LVDT). A number of strain gauges were installed on the GFRP wrap to record the hoop strain around the diameter of the pole and along its length. Other configurations of the strain gauges were used in Phases II and III, which are explained in detail the next chapters. All of the deflection and strain readings were recorded on a National Instruments data acquisition system.

The test configuration, Figure 7, is inverted compared to the actual loading and support configuration for practical purposes, although the bending moment diagram is identical. The bearing surface of the loading piece was 10.2 cm by 16.5 cm. The diameter of the pin shown to the right of Figure 7 was 2.2 cm. Finally, the bearing surface of the roller support on the timber was 10.2 cm by 20.3 cm.

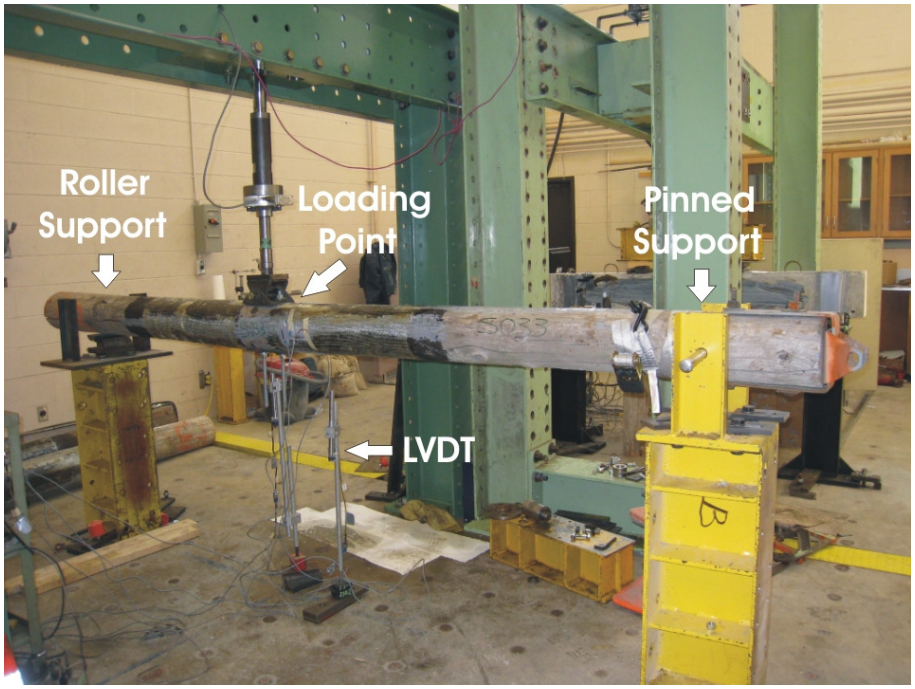

Figure 7: Laboratory Setup

3.3 Strengthening System

This section presents the major components of the proposed strengthening system. These components include the surface preparation consisting of sanding the surface and filling the cracks, and application of the GFRP wrap. These components were investigated as variables in different phases of the testing program of this thesis.

3.3.1 Sanding the Surface

Sanding the surface was the first step in the proposed strengthening system. The surface of the specimens was heavily deteriorated, in particular on the top half of the specimens, where they were exposed to direct rain and sunlight. In order to provide a smooth surface for the application of the GFRP wrap, the samples were sanded to a depth of 3-5 mm using an electric sander.

3.3.2 Crack Filling

The surface cracks or splits in the specimens reached 20 mm in surface width in some cases and normally extended to the middle core of the sample. All of the cracks that existed in the areas that were to be wrapped were filled using SikaAnchorFix-3. This filler is a two part black and white epoxy, that was mixed together to achieve a constant gray viscous epoxy with a set time of only five minutes. The material properties of SikaAnchorFix3 are summarized in Table 2. These values are based on the Product Data Sheet Edition 07.2007 from Sika Canada.

Table 2: Material Properties for SikaAnchorFix3

Compressive Strength	Compressive Modulus	Ultimate Elongation	Bond Strength (14 days)
75 MPa	3656 MPa	1%	75 MPa

Due to the large width of the cracks, the cracks were easily filled using a trowel and crack injection was not required. In Figure 8, the filler has been extended beyond the wrap to show a side by side comparison of the filled and unfilled portions of a crack. The cracks were completely filled, which both prevented the opening of the cracks during loading and provided a solid surface for the application of wrap. In the samples that were not crack-filled, there were numerous air pockets under the wrap due to the trapped air in the cracks.

Figure 8: Filler Material

3.3.3 GFRP Wrap

Glass Fibre Reinforced Polymer wrap was selected for the proposed strengthening system. The stiffness of the GFRP wrap is lower than the CFRP wrap, which makes it more compatible with wood applications. SikaWrap Hex 100G, a unidirectional E-glass fibre fabric, was used for this research program. This material was laminated using Sikadur Hex 300, which was a two part clear colour epoxy, also made by Sika. Table 3 summarizes the fibre properties of SikaWrap Hex 100G.

Table 3: SikaWrap Hex 100G Material Properties

Tensile Strength	Tensile Modulus	Elongation	Density	Area Weight
2.3 GPa	72 GPa	4%	2.55 g/cm^3	915 g/m^2

Table 4 summarizes the cured laminate properties of SikaWrap Hex 100G laminated with Sikadur Hex 300 epoxy, cured at 21°-24°C for five days. All the values in this table are the

average values published by Sika and differ from the suggested design values, which could be found on the Product Data Sheet for SikaWrap Hex 100G edition 07.2007.

Table 4: Cured Laminate Properties of SikaWrap Hex 100G

Tensile Strength	Tensile Modulus	Tensile % Elongation	Compressive Strength	Compressive Modulus	Ply Thickness
612 MPa	26119 MPa	2.45%	597 MPa	29715 MPa	1.016 mm

3.4 Sample Preparation

There are two types of application procedures for FRP wraps: wet layup and dry application. Sika Canada recommends the wet layup for GFRP products as the saturation of the wrap was deemed an essential part of the application process. In contrast to CFRP wrap, GFRP wrap absorbs a significant amount of epoxy, and therefore the dry layup of GFRP could lead to unsaturated areas in the laminated wrap, which would cause local weak regions in the strengthening system. Therefore, the processes explained in the following paragraphs refer to the wet layup that was used in the experimental program of this thesis.

The first step in the wet layup process was the application of Sikadur 300 epoxy to the surface of the specimen. Figure 9 shows the application of the epoxy to the surface of the pole. The epoxy was applied using a paint roller to achieve a uniform application of the epoxy. The pole samples that were not sanded absorbed most of the epoxy on the first coat and therefore a second coat was required. The epoxy was left on the surface for approximately 20 minutes to achieve a tacky texture. The application of the epoxy to the surface served two purposes: bond enhancement between the wrap and the surface as well as preventing the absorption of the epoxy in the saturated wrap into the surface, and thus keeping the wrap saturated during curing.

Figure 9: Epoxy Application to Cross-arm Surface

Figure 10 shows the "saturation bed" that was prepared for the GFRP wrap pieces. The purpose of the saturation bed was to ensure that the GFRP wrap was completely saturated prior to the application on wood. The bed needed to be slightly larger than the surface of the wrap to ensure that wrap could be laid out flat. The 2" by 4" wood pieces around the bed were placed to ensure that the epoxy was contained in the saturation bed.

In industrial applications, the GFRP wrap is soaked in an epoxy bath to ensure full saturation. However, for the purposes of lab application and due to the limited number of fabric pieces, the epoxy was applied to the wrap as shown in Figure 11. The process shown in this figure was repeated for both sides of the wrap. The GFRP wrap became completely transparent when it was fully saturated. The saturated wrap was then applied to the specimen as shown in Figure 12.

Figure 10: Soaking Bed for GFRP Wrap

Figure 11: Saturation of GFRP Wrap

The wrap was applied and tightened around the circumference of the member by pulling the wrap as it was being applied. An overlap of approximately 250 mm was recommended by Sika to ensure that proper bond was developed to utilize the full capacity of the confinement.

Figure 12: Application of GFRP on the Cross-arm

After the initial application of the wrap to the surface, the air bubbles that were formed under the wrap were "massaged out" as much as possible. The 250 mm of overlap was also placed on top of the specimen to ensure that the saturated wrap did not pull off under its own weight. The wrap was re-tightened by hand approximately 30 minutes after the initial application to make sure it fit snugly on the specimen.

The samples were then kept in a well ventilated room for three days, after which the epoxy was completely hardened. At that time the samples were moved to the lab area, where they were kept for another 4 days to ensure that seven day required curing time was met. The strain gauges were installed on the wrap in different configurations as detailed in the next chapter of this thesis, and then the samples were tested to failure in three point bending.

3.5 Phase I: Feasibility Study

Phase I was designed and conducted to test the feasibility of the proposed strengthening system. Since this strengthening system was not implemented before, it was critical to have an estimate of the expected strength gain through the application of this strengthening system.

The experimental program consisted of six cross-arm specimens removed from existing Gulfport structures in Ontario. Three samples were tested as control specimens with no strengthening, and the other three were strengthened using the GFRP Wrap. Details of all specimens are summarized in Table 5. Strengthened specimens S2 and S3 were wrapped 1.2 m on each side of the loading point, while S1 was wrapped only 0.6 m on each side of the loading point. The wrap was placed with the fibres perpendicular to the axis of the member.

Table 5: Phase I Specimen Specifications

Specimen	Diameter[1] (mm)	Initial Wood Condition	Wrap Width	Surface Prep.
C1	232	Many wide and deep cracks along the length, a number of wide cracks at each end	None	None
C2	264	A number of small cracks along the length, no sign of significant deterioration.	None	None
C3	229	A number of small cracks along the length, no sign of significant deterioration.	None	None
S1	277	Small to medium size cracks	0.6 m	Sanded Crack Filled
S2	283	Many wide and deep cracks along the length, wide cracks at each end	1.2 m	Sanded Crack Filled
S3	286	Small to medium size cracks along length, generally good condition	1.2 m	Sanded Crack Filled

[1] - Diameter at the loading point

3.6 Phase II: Parametric Optimization

The results from the initial phase of the experimental program are presented in Chapter 4. Based on the findings of Phase I, the proposed strengthening system was estimated to increase the load carrying capacity of the cross-arm members by approximately 42%. The strength gain was significant and deemed sufficient for the load carrying capacity that was required by Gulfport Structures. Therefore, Phase II of the testing program was designed in order to test the different variables and configurations to reach the optimal parameter configurations for the proposed strengthening system.

There were seven factors that could potentially have an impact on the performance of the proposed strengthening system, as detailed later in this section. A full factorial experiment that would cover all the factors would require 128 experiments, while each sample required approximately five days of lab work from the preparation to final testing. Therefore, approximately 900 days of continuous lab work would be required to investigate the effect of all factors. Due to the large number of required experiments, the factors were reduced to 4, which still would require 16 experiments and 90 days of continuous lab work. Managing this many samples during only one phase of a Master's project was still not feasible, and therefore alternatives for designing a more efficient testing program were investigated.

Taguchi Methods and Analysis of Variation (ANOVA) were used to achieve the most efficient testing program. In addition to reducing the number of required samples, these tools provide many advantages over traditional full factorial and partial factorial experimental designs. Taguchi Methods and ANOVA are explained in the next section to provide the reader with a basic background on the methods. However, these explanations are not meant to be used as instructions for applying the methods, and the reader is strongly encouraged to review the references that are presented at the end of this thesis for further explanation of the methods and application guidelines.

3.6.1 Taguchi Method

Taguchi method was first developed by Professor Genichi Taguchi as an offline quality control system for the automotive industry (Dehnad 1988). It was then introduced to other disciplines as an offline quality control system and later become an effective tool in the design of experiments. The Taguchi method allows for the determination of the optimum parameters by analyzing the variability that is caused in the system due to those factors (Barker 1990). In other words, the sensitivity of the system to each variable is analyzed and compared to the effect of other factors as well as to the effect of the natural error of experiment.

Taguchi is most known for his contributions to the quality control industry. The design of experiments is only one aspect of his more general quality control method. The Taguchi method uses the optimal design of experiments to find the most effective factors through analysis of variation, and then analyses the effect of other noise factors through signal to noise ratio, in order to be able to both design for the target value as well as to minimize the sensitivity of the system to noise factors. For the purposes of the experimental design of this thesis, only the parameter design aspect has been utilized for the reasons discussed in the next section. Therefore, the explanations and methods of analyzing and dealing with Signal to Noise ratio are not presented in this thesis.

In order to understand the methodology behind the Taguchi Design, some basic understanding of the terminology, fundamentals of experimental programs, and a number of statistical facts need to be introduced. The following sections of this chapter aim at introducing these concepts that are built into the Taguchi method, prior to introducing the method itself.

In Taguchi terminology, “factor” refers to a variable that can be controlled or monitored, and available “levels” refer to the number of potential values or configurations that are available for a particular factor (Barker 1990). The same terminology has been used in this thesis in

order to maintain consistency with other sources. For example, the application of the filler material is a two-level factor in this research program, as it can take two potential configurations: applied and not applied. Also, the degree of freedom that a variable requires in the experimental program is equal to the number of levels minus one. In the above example, the filler material requires a degree of freedom of one. This concept is explained in more detail in the following sections.

3.6.1.1 Control Factors vs. Noise Factors

The results of any experiment can be evaluated by the value of the response parameter as well as its variation. The less variable the data, the more reliable the results would be. The factors that are responsible for the value as well as the variability of the response variable can be divided in two categories: control factors and noise factors (Bendell et al. 1989).

Control factors are those that can be controlled and varied at reasonable cost and effort. For example, in the proposed strengthening system the width of wrap, sanding the surface, and use of filler material are control factors. However, noise factors are not in the control of the experimenter, or may be physically or financially not feasible to control. In this particular application, the noise factors would be the temperature, humidity, and sun exposure during the curing and the expected life of the strengthening system. Other factors such as the level of the internal rot and the original strength of the wood are also considered as noise factors in this research.

Control factors can be optimized using the Taguchi Method through Orthogonal Arrays, as discussed later in this chapter. The optimization of the control factors sets the target value, in this case the failure load, for the specimen. However, noise factors are responsible for variability within the data, and the variability also needs to be minimized in a well designed product or system. Although it is not possible to design the optimal noise factors because they cannot be controlled or specified, it is possible to design the control factors so that the effect of noise factors is minimized. This can be achieved by incorporating a nested

orthogonal array within the original orthogonal array; the nested array would include the noise factors, while the main array includes the control factors. Analysis of Signal to Noise ratio would then determine the optimal configuration for minimizing the variability within the data.

For the purposes of this research program, testing under various noise factors was not feasible at the available laboratory facilities, as temperature or moisture controlled environments were not available. However, the factor D, surface deterioration, has been included to represent a noise factor even though it has been implemented as part of the main array. The reason that this particular noise factor was studied was that if the strength values were found to be independent of the level of surface deterioration, the need for an extensive conditional assessment of the structures would be eliminated. Therefore, the proposed strengthening system could be applied more consistently and more uniformly on most structures regardless of their initial condition.

3.6.1.2 Process Flow Diagram

The first step in applying the Taguchi method is to understand the processes that need to be optimized. The strengthening system consists of a series of processes, which are described in the flow chart in Figure 13. This research focuses on the effect and the necessity of each of these processes to determine which processes can be eliminated or improved in order to achieve a more practical and efficient strengthening system design. The flow chart in Figure 13 is an example of a preliminary overview of all of the processes that are involved, which may differ significantly from the final proposed strengthening system.

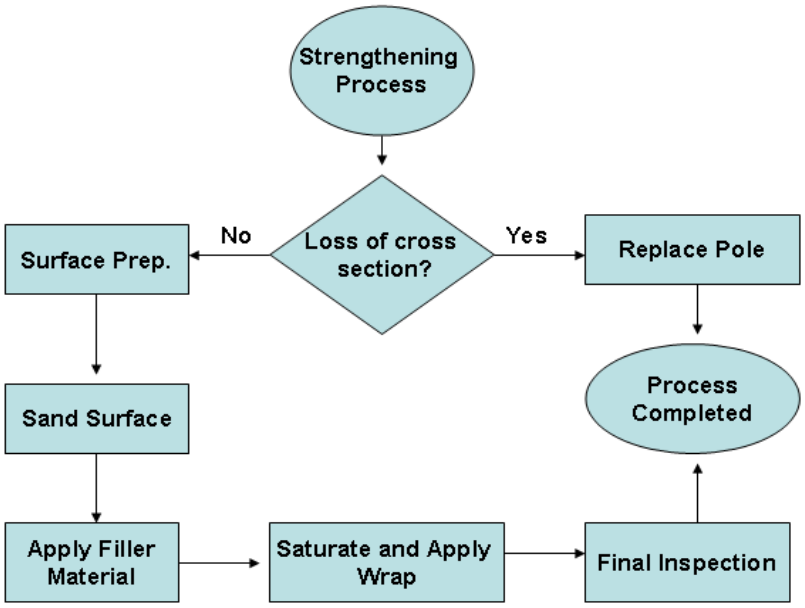

Figure 13: Process Flow Diagram

3.6.1.3 Cause and Effect Diagram

The factors as well as their respective levels that could potentially impact the overall quality of the strengthening system are shown in the cause and effect diagram in Figure 14. The overall objective was to achieve a "High Performance Strengthening System". The factors and levels identified could be altered to impact this objective. The purpose of Phase II of the experimentations was to analyze the effect of each variable at their different levels and design the optimum configuration of these factors to achieve the highest performance in the strengthening system. Therefore, Phase II was a parameter optimization problem, which proved to be very suitable for the application of the optimization techniques of Taguchi.

The cause and effect diagram in Figure 14 included all seven factors and their respective levels. From the seven factors in this figure, type of wrap, FRP strip (applied on the tension side), and number of layers were eliminated as it was assumed that one layer of unidirectional GFRP wrap with no FRP strip was the weakest combination of these factors. If

the minimum combination was deemed adequate, which was confirmed in Phase I, then there would be no need of introducing other factors that would complicate the installation and increase the implementation cost of the proposed strengthening system.

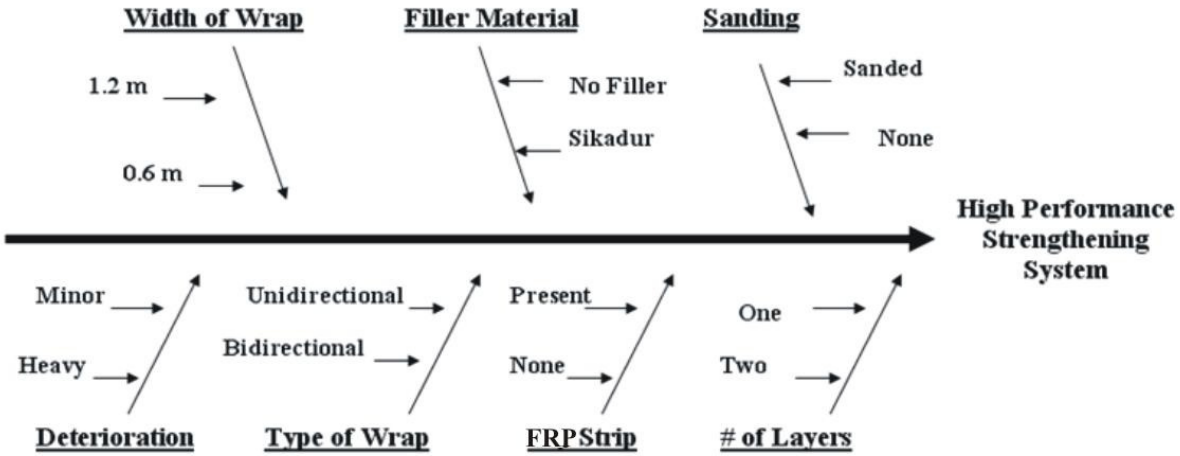

Figure 14: Cause and Effect Diagram

3.6.1.4 The Interaction Effect

The world's most common experimental design is the "vary one factor at a time" design (Batish 2007). In this type of experiments all factors are kept constant while one factor changes from one experiment to the next. The interaction effect is best described through the use of an example. Let us assume that a researcher is investigating different factors that are believed to impact the amount of corrosion in the reinforced concrete beams. The factors that are being analyzed are: A (concrete cover), B (strength of concrete), C (amount of air content) and D (exposure time). Table 6 summarizes the levels of the two factors A and D, which are discussed in the following paragraphs.

Table 6: Factors Involved in Interaction Example

Factor	Description	Level 1	Level 2
A	Concrete Cover	20 mm	50 mm
D	Exposure Time	30 days	120 days

In Table 7, the researcher is looking for the effect of Factor D, so two samples are prepared with all variables staying constant while Sample I includes factor D at level one (30 days exposure) and sample II includes factor D at level 2 (120 days exposure). The results show that the amount of load carrying capacity of the beam was increased by 50% when the exposure was reduced from 120 days to 30 days, and thus the exposure time played a significant rule in this case. However, this observation is potentially inaccurate due to the poor experimental design as explained below.

Table 7: Interaction Example (Experiment 1)

Sample	A	B	C	D	Load
I	1	1	1	1	75 kN
II	1	1	1	2	50 kN

In the above example all factors have been kept at their first level. Now consider the experimental program in Table 8, again aimed at determining the effect of factor D. In this case factors B and C are still kept at level 1, while factor A is kept at level 2 instead of 1.

Table 8: Interaction Example (Experiment 2)

Sample	A	B	C	D	Load
I	2	1	1	1	80 kN
II	2	1	1	2	79 kN

Theoretically, experiment 1 and experiment 2 should yield similar results as all factors are kept constant, while factor D has been changed from sample I to sample II. However, as you can see the effect of factor D on the load carrying capacity of the sample has been reduced from 50% to 1.3%! This argument can be made for factors B and C as well. In this case, when factor A is kept at level 2 which corresponds to 50 mm of cover, the bars would not corrode even in 120 days, so changing the exposure from 30 days to 120 days has minimal impact on the strength of the sample. In this case factors A and D are interacting with each other and the effect of neither one can be investigated individually. Although the "one factor at a time" design is the world's most common experimental design, it is also the world's worst experimental design due to its inefficiencies as well as its lack of ability to catch the interaction effect (Batish 2007).

As shown by the above example the design of the experiment can make crucial impacts on the results of an experimental program. Therefore, in order to achieve an efficient as well as an accurate experimental program, the Taguchi method has been used for designing Phase II of the experimental program of this thesis. The next sections of this chapter cover the basics of the Taguchi method and the details of the experimental program of Phase II.

3.6.1.5 Taguchi Method and Design of Experiments

The experimental design portion of Taguchi method is based on the analysis of variation (ANOVA). An experimental program needs to meet certain criteria in order to be able to produce statistically accurate and reliable results.

The interaction effect needs to be included in any well-designed experimental program. As explained in previous sections, ignoring the interaction effect can lead into very misleading results. In addition to the interaction effect, another important aspect of a well-designed experimental program is its orthogonality. The concept of orthogonality requires the same number of observations under all levels of a given factor (Roy 2001). For example if there are four observations under level one of factor A, there needs to be four observations under

level two of factor A. This concept has to be applied to all factors in the experimental program. Also, if there are two factors involved and both have two levels, then the number of observations under A1-B1 has to be the same as A1-B2 and so on. The experimental program shown in Table 9 is an example of a completely orthogonal experiment.

Table 9: Orthogonal Experiment

	A-1	A-2
B-1	4 observations	4 observations
B-2	4 observations	4 observations

Taguchi has used these criteria, in addition to other statistical concepts, to design a number of predefined experimental designs that could be used by researchers depending on the type and number of factors involved. Taguchi also has provided methods for modifying these predefined designs to fit into most experimental programs. These predefined experimental designs can be used to choose, modify, and perform the most efficient testing program. After the experiments are conducted, the analysis of the results needs to be conducted using ANOVA as explained in the next chapter of this thesis.

3.6.1.6 Orthogonal Arrays

The predefined experimental designs are referred to as Orthogonal Arrays (OA) in Taguchi terminology. The orthogonal arrays have been designed for two major classes of factors: two level factors and three level factors. The orthogonal arrays for two level factors are: OA4, OA8, OA16, OA32, etc, while the orthogonal arrays for three level factors are: OA9, OA18, OA27, etc (Roy 2001). The number following the OA refers to the number of observations that are required in that particular orthogonal array. The number of available degrees of freedom in each OA is equal to the number of experiments minus 1. On the other hand the number of required degrees of freedom by each factor is equal to the number of its levels minus 1. Therefore, seven two-level factors can theoretically be analyzed using an OA8 with

only 8 experiments. However, it is always a good idea to leave one degree of freedom for error. The function of an error column is to measure the degree of variability due to natural causes of variation within the experimental program. Therefore, if a significance of a given factor is lower or even slightly higher than the significance of the error column, the effect of that factor is statistically insignificant. These concepts are presented in the next chapter for the ANOVA analysis.

A standard OA8 experimental design is shown in Table 10. In this table the first column refers to the number of observations, therefore there are eight observations required. Any factor, interaction, or the error can be assigned to columns C1 through C7, as discussed earlier. The numbers in the table (1 or 2) refer to the level of the factor assigned to that column. For example, in order to prepare observation 1, all factors have to be kept at level 1, while in observation 2 only the factors assigned to columns C1, C2, and C3 are kept at level 1 and others switched to level 2.

Table 10: Orthogonal Array (OA8)

Observation	C1	C2	C3	C4	C5	C6	C7
1	1	1	1	1	1	1	1
2	1	1	1	2	2	2	2
3	1	2	2	1	1	2	2
4	1	2	2	2	2	1	1
5	2	1	2	1	2	1	2
6	2	1	2	2	1	2	1
7	2	2	1	1	2	2	1
8	2	2	1	2	1	1	2

The Taguchi method specifies the assignment of the factors to the different columns using tables or design triangles; the latter was used for this experimental program. The procedure for assigning the factors to columns is beyond the scope of this thesis and readers are encouraged to refer to Wynn and Logothetis (1989) or Batish (2007). However, it is important to note that if there were no interactions to be considered then the factors and the error column could be arbitrary assigned. However, when interactions are included then the

assignment becomes more complicated and either the design tables or design triangles need to be used to assign the interactions to the correct columns.

Table 11 shows an OA9 experimental design. As explained earlier OA8 is based on two-level factors while OA9 is based on three-level factors. OA9 has fewer columns than OA8, despite having an extra observation. The reason for the fewer columns is that each column has three levels, thus allowing for three level factors. In the OA9 experimental design, each column has a degree of freedom of 2 and therefore the total degrees of freedom are 8. Therefore, 4 factors each at three levels can be analyzed using this design.

Table 11 - Orthogonal Array (OA9)

Observation	C1	C2	C3	C4
1	1	1	1	1
2	1	2	2	2
3	1	3	3	3
4	2	1	2	3
5	2	2	3	1
6	2	3	1	2
7	3	1	3	2
8	3	2	1	3
9	3	3	2	1

There may be some cases in which the researcher would like to use a mix of two-level, three-level, or even four-level factors. Taguchi offers a number of methods to tailor the predefined experimental design to the needs of the experimenter including:

- Merging Column: A four-level factor can be fit into a two-level OA
- Dummy Treatment: A three-level factor can be fit into a two-level OA
- Combination Method: Two-level factors can be fit into a three-level OA
- Idle Column Method: Many three level factors can fit into a two-level OA (Roy 2001).

The discussions of these methods are beyond the scope of this thesis as such methods were not employed in the experimental program of this research. However, full descriptions along with examples are provided in most of the references on this topic (Roy 2001).

3.6.1.7 Analysis of Variation (ANOVA) and F-test

All experimental programs aim at controlling the target value as well as the variation of a particular product or process. Analysis of variation (ANOVA) can be used as a statistical method to interpret data and make decisions and conclusions with respect to the effect of parameters involved in a given experimental program. There are many levels to ANOVA starting from no-way ANOVA, which includes no control factors. An example of no-way ANOVA is taking repetitive random measurements of a certain product from a production line. Higher order ANOVA analysis can take into account many different variables. The experimental program of this research, which has been designed using Taguchi Method, is analyzed using higher order ANOVA.

The variation in the data could either be from the control factors, noise factors, or the natural error of experimentation. Therefore, a comparison between the variation due to a certain factor and the variation due to error of experimentation is more meaningful than an absolute value of variation due to a factor. For example, if the variation due to the error is greater than the variation due to any other factor, regardless of the actual value of variation due to that particular factor, the effect of that factor is statistically insignificant. In order to provide for a systematic relative analysis of variation the F-Test was used, which is simply a ratio of sample variances. In ANOVA calculations, this ratio is taken as the ratio of the variance of a certain factor to the variance of the pooled error. These concepts are further explained in the next chapter of this thesis, which deals with experimental results. The equations, methodology, and results are explained in that chapter.

3.6.2 Phase II Experimental Program

The factors and their corresponding levels that have been investigated in Phase II of this experimental study are listed in Table 12. In addition to the factors listed, two interactions of these factors were also studied: surface deterioration and width of wrap in addition to surface deterioration and filler material.

Table 12: Factors and their Corresponding Levels in Phase II

Level	Deterioration (D)	Width of Wrap (A)	Filler Material (B)	Sanding (C)
1	Minor	1.2 m	None	No
2	Heavy	0.6 m	Anchorfix-3	Yes

In Table 12, the factor D refers to the surface deterioration and is not directly related to the internal deterioration of the member. The testing program was originally setup to investigate the effect of internal rot or deterioration; however, only one sample with severe internal rot was received, and thus only the effect of surface deterioration was studied. Also, for the purposes of a visual inspection, the surface deterioration is much easier to investigate than the internal deterioration of the member. Factor A refers to the width of the GFRP wrap. The two wrapped areas on both sides of the brace connection use the same level of factor A, as indicated on the table above. Factor B indicates whether a filler material was used or not. Level 2 of factor B refers to the presence of the filler material. Sika AnchorFix-3 was used as the filler material and was applied thoroughly to fill-in all of the surface cracks and therefore prevented the cracks from opening during loading. Finally, the two levels of factor C indicate whether the surface has been sanded or not. Sanding the surface was done using an electrical sander, which penetrated 3-5 mm into the surface of the specimens.

According to the number of factors and interactions that were considered, an Orthogonal Array (OA-8) was used to provide sufficient degrees of freedom for this experimental program. Six degrees of freedom were used for the factors and their interactions and one degree was used for error, which proved to be very important in this study, as explained

through ANOVA analysis in the next chapter. The assignment of the factors, their interactions, and the error to the columns of the OA-8 experimental program are summarized in Table 13. In order to minimize the error of experiment the samples were prepared and tested in a random fashion and not in the order that is presented in the table.

Table 13: Orthogonal Array (OA8) for Phase II

Observation	C1 D	C2 A	C3 D&A	C4 B	C5 D&B	C6 Error	C7 C
1	1	1	1	1	1	1	1
2	1	1	1	2	2	2	2
3	1	2	2	1	1	2	2
4	1	2	2	2	2	1	1
5	2	1	2	1	2	1	2
6	2	1	2	2	1	2	1
7	2	2	1	1	2	2	1
8	2	2	1	2	1	1	2

The experimental design outlined in Table 13, is described in words in Table 14. In this table the numbering system is replaced with the appropriate terms corresponding to those numbers. The columns that were assigned to error and interactions are taken out in this table, as they have no physical meaning in terms of sample preparation and are only used for calculation purposes.

Table 14: Specimen Description for Phase II

Observation	Deterioration	Width of Wrap	Filler Material	Sanding
1	Minor	1.2 m	None	None
2	Minor	1.2 m	AnchorFix3	Sanded
3	Minor	0.6 m	None	Sanded
4	Minor	0.6 m	AnchorFix3	None
5	Heavy	1.2 m	None	Sanded
6	Heavy	1.2 m	AnchorFix3	None
7	Heavy	0.6 m	None	None
8	Heavy	0.6 m	AnchorFix3	Sanded

3.7 Phase III: Confirmation Testing

The purpose of the second phase of testing was to identify the most critical factors, their impact on the strengthening system and finally the optimum configuration of the parameters. Using ANOVA analysis and the Orthogonal Arrays, it was also possible to estimate the mean and a confidence interval for the strengthened specimens, given that they were strengthened using the optimal configuration.

The purpose of Phase III was to confirm the estimated mean and confidence from Phase II. Therefore, three specimens were prepared and were all strengthened using the optimal configuration that was obtained from Phase II. This optimal configuration was: not sanding the surface, filling the cracks with Sika AnchorFix3, and using 0.6 m wide GFRP wraps. These three samples were tested to ensure sufficient data to confirm the confidence interval that was calculated based on the results of Phase II.

3.8 Material Testing

Material testing was conducted to compare the material properties of aged specimens with the published values for new specimens. Small clear samples were obtained from the middle core of the cross-arms to obtain material properties. Most of the cross-arms were treated with creosote in order to increase their durability. The presence of the creosote limited the sampling of the cross-arms to the middle core of the members. Two types of material testing were conducted: Shear-Parallel-to-Grain and Compression-Parallel-to-Grain. A moisture content test was also conducted on all specimens from both tests, as the material properties of timber are known to be very dependent on the moisture content of the samples.

3.8.1 Shear-Parallel-to-Grain-Test

The shear-parallel-to-grain test was conducted in accordance with the Standard Test Methods for Small Clear Specimens of Timber (ASTM: D143-94 [Reapproved 2007]) with minor

adjustment in the size of the samples. The samples that were made for the shear parallel to grain test were 5.08 by 6.35 by 5.08 cm [2 by 2.5 by 2 in] and notched to produce failure on a 5.08 by 6.35 cm plane instead of the 5.08 by 5.08 cm plane recommended in the standard. The loading configuration of this test is schematically shown in Figure 15. The picture to the left shows the loading on the sample prior to failure, and the picture to the right shows the failure mechanism of the sample.

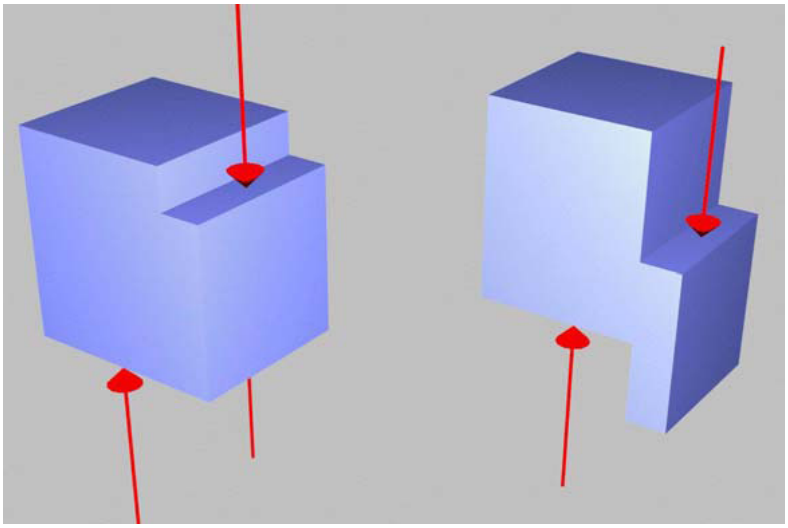

Figure 15: Loading Configuration for Shear Parallel to Grain Test (Ho 2005)

The test sample and testing apparatus, which was previously designed at University of Waterloo based on ASTM standards, are shown in Figure 16. In this figure the sample is shown from the side, where it is held in place using the apparatus as shown, and a ¾" plate is pushing down on the notched section to produce a failure. A total of 29 samples were tested for shear parallel to grain.

The test was conducted on a 100 kN capacity MTS frame in the structural laboratory of University of Waterloo, and the load was applied continuously throughout the test at a rate of 0.6 mm/min, as per the ASTM standard. The sample was tested to failure and then the

moisture content was obtained. The results of this test, along with the moisture contents, are compared to the published values for the same species of wood.

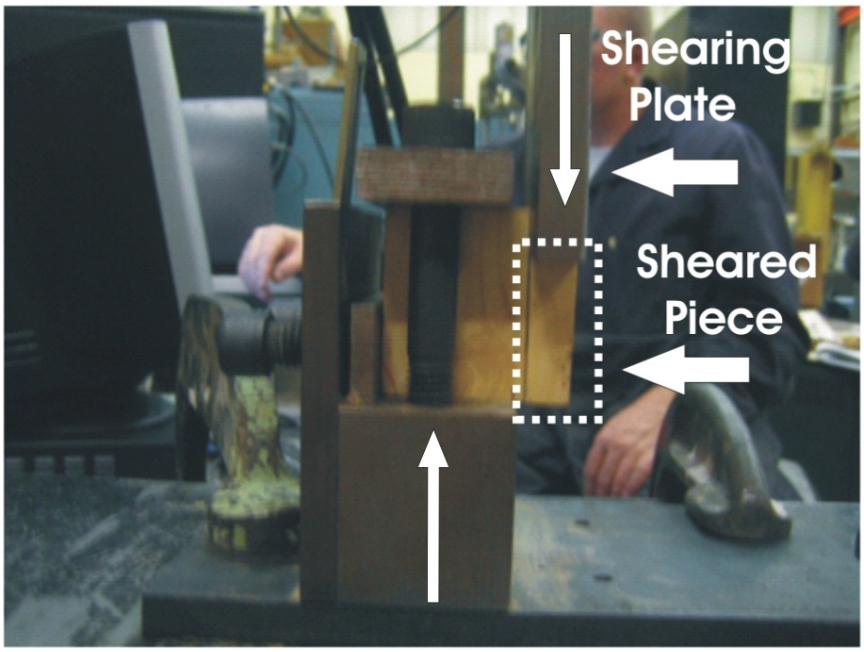

Figure 16: Shear Test Setup

3.8.2 Compression Parallel to Grain Test

The compression-parallel-to-grain test was conducted in accordance with the Standard Test Methods for Small Clear Specimens of Timber (ASTM: D143-94 [Reapproved 2007]) without any changes or modifications. The samples were 5.08 by 5.08 by 20.32 cm [2 by 2 by 8 in.] and were cut from the clear sections that did not have any creosote, deterioration or any major cracks. The samples were tested using a servo-hydraulic testing frame, with the load being applied continuously at a rate of 0.6 mm/min, as per ASTM specifications. The test configuration and setup are shown in Figure 17. The horizontal beam in this figure was part of the testing frame and was equipped with a spherical seat to provide a uniform load across the top surface of the specimen.

Figure 17: Compression Parallel to Grain Test Setup

The loading piece in Figure 17 is equipped with spherical bearing to obtain uniform distribution of load over the specimen. There were a total of 14 specimens tested for compression-parallel-to-grain and there were all tested for moisture content after the test. The results of the tests as well as moisture contents are reported in the next chapter and compared to the published material properties for this type of wood.

4 Experimental Results and Analysis

The experimental results and analysis of the three phases of this research program are presented in this chapter. Since the experimental program was conducted in three separate phases, with each phase designed to investigate different research objectives, the results and analysis are presented for each phase individually. The first three sections of this chapter present the three separate phases of the testing program. Material testing is also presented in this chapter in a separate section.

4.1 Phase I: Feasibility Study

The main objective of Phase I of the experimental program was to analyse the effectiveness and feasibility of the proposed strengthening system on the Gulfport cross-arms. Due to the lack of published literature on strengthening circular and deteriorated timber elements, the results from this phase of testing were required to justify an extensive research project on the proposed strengthening system.

The properties of wood are highly dependent on its moisture content, growth environment, and even the length of summer months during growth years (Ho 2005). Therefore, highly scattered data were expected for the control samples. In order to be able to present reliable and representative data, it was decided to test three control samples and compare them to three strengthened samples. The comparison was done in terms of the average of each group to minimize the effect of variability of the data as much as possible.

The three strengthened samples in this phase were all sanded to a depth of 3-5 mm using an electric sander to provide a smooth surface for the GFRP Wrap. In Figure 18, the specimen on the left was not sanded, while the one on the right side was sanded. As can be seen in these photos, the sanding process minimized the cracked and roughened surface and provided

a smooth surface for the application of the wrap. All of the surface cracks that were wider than 2 mm were filled using the Sika Anchorfix 3.

Figure 18: Sanding Effect

Table 5 summarizes the details of the six specimens that were tested in Phase I of the experimental program. Samples C1-C3 were control samples and S1-S3 were strengthened using the GFRP wrap. Sample S1 was wrapped using GFRP wraps with a width of 0.6 m on each side of the loading piece, while samples S2 and S3 were wrapped with GFRP wraps with a width of 1.2 m on each side of the loading piece to assess the effect of doubling the width of the wrap. The samples were tested in three-point bending as described in the previous chapter of this thesis. The deflection of the beam at four points was measured using Potentiometers and LVDTs. One deflection reading was obtained at the mid-span of the member and two others were taken half way from each support to the mid-span. The fourth reading was taken under the loading point.

Table 15 summarizes the overall experimental results for all specimens. The maximum load refers to the highest load that was recorded by the load cell and corresponds to the failure load of the member. The deflection value that is listed on the table refers to the deflection of

the member under the load point, which was not necessarily the maximum deflection of the member, but very close to it.

Table 15: Phase I Experimental Results

Specimen	Effective E (MPa)	Maximum Load (kN)	Deflection (mm)	Bending Stress (MPa)	Failure Mode
C1	5.65	41.7	24.6	23.5	Split at the pin support
C2	3.80	82.6	37.9	31.7	Combined Shear & Flexure
C3	3.58	49.2	42.5	29.0	Combined Shear & Flexure
S1	5.66	135.6	35.7	45.3	Split at the pin support
S2	3.65	106.0	51.2	33.0	Flexure-Tension
S3	6.77	137.2	59.0	41.4	Flexure-Tension

The bending stress at failure is also presented in Table 15, calculated as the stress in the outer fibres of the member. Finally, the effective Modulus of Elasticity (E) is calculated using Equation 1. $E_{effective}$ is intended to provide a comparative measure of the material stiffness, and it should not be compares with published "E" values. Equation 1 is a modified deflection formula for a point load (P) applied on a simply supported beam.

Equation 1: $$E_{effective} = \frac{P \times a^2 \times b^2}{3 \times \Delta \times L \times I}$$

where P is the load, Δ is the deflection at load P, a and b are the distances from the supports to the load P, L is the total length of the member, and I is the moment of inertia of the member at the loading point.

Figure 19 illustrates the Load-Deflection behaviour of each specimen up to the point of failure. As shown in this figure, most of the strengthened specimens follow a more ductile behaviour than the control ones. Sample S1 was an exception to this observation. This sample had one of the highest loads among all Phase I specimens, but had significantly lower deflection in comparison to the other strengthened specimens as well as some of the control

ones. This difference in the deflections is explained through the discussions of the failure modes in the next two sections.

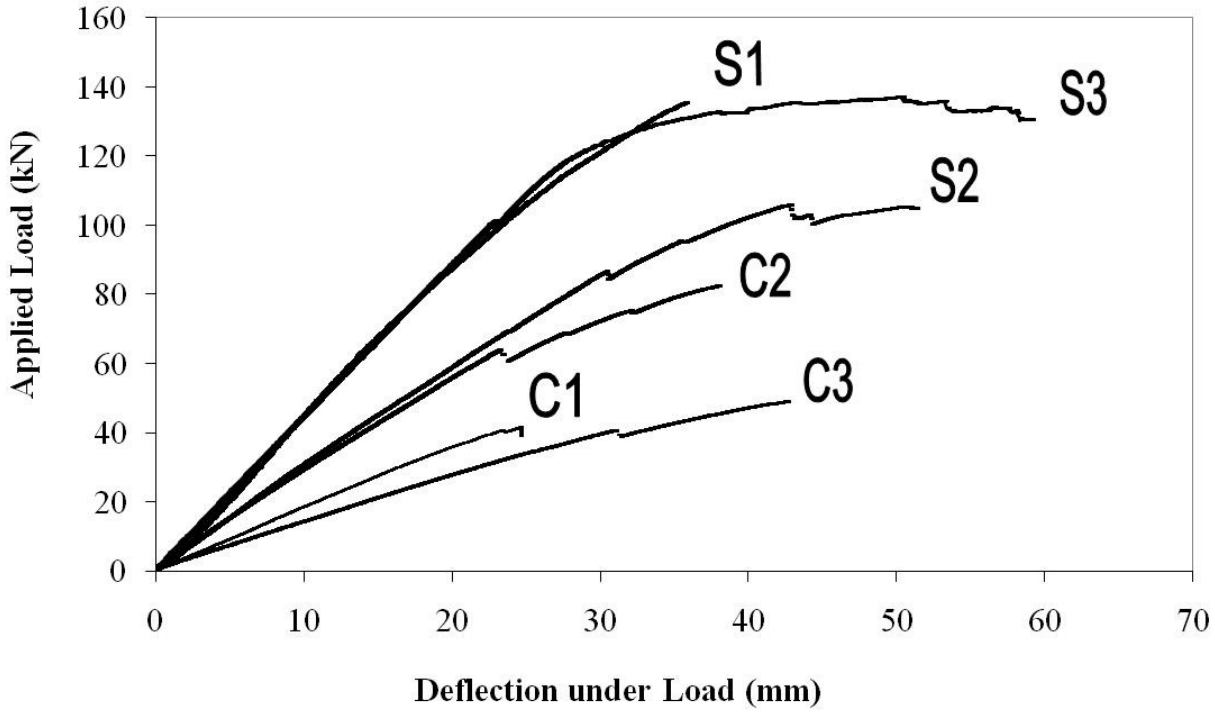

Figure 19: Load-Deflection Behaviour of all Specimens in Phase I

4.1.1 Combined Shear-Flexural Failure

Most of the control specimens failed under combined shear-flexural mode. The failure was originated by horizontal shear cracks on the bottom half of the specimen, approximately 20 cm to each side of the loading piece. The cross-section of the specimen at the loading point, and thus the maximum moment region, was reduced due to the presence of the shear cracks, which then caused the flexural cracking and failure of the specimen. Figure 20 shows a typical combined shear-flexural failure. Figure 21 shows a typical horizontal shear crack. In

some specimens, the shear crack was more evident, such as the specimen shown in Figure 21, while in other specimens the flexural cracking was more obvious, as shown in Figure 20.

Figure 20: Combined Shear-Flexure Failure (Left: Side View – Right: Bottom View)

Figure 21: Typical Failure of Control Specimens

4.1.2 Splitting Failure at Pinned End

One control specimen and one strengthened specimen failed by splitting of the member at the pinned end. Figure 22 shows this type of failure mode for these two samples. The pictures on the left side show the specimens before the test and the pictures on the right side show the failed specimens. Both specimens had experienced noticeable deterioration on the areas that were split open, although the cross-section was not significantly reduced due to that deterioration. Most of the deterioration was present at the bottom of the deep cracks that extent from the surface to close to the middle of the specimens.

Figure 22: Splitting Failure at Pinned Support

Figure 23 shows the side view for the strengthened specimen that failed by splitting at the pinned end. This specimen was wrapped using the shorter width (0.6 m) of GFRP wrap. The samples with the full width of GFRP wrap did not experience any failure at the pinned end.

Figure 23: Splitting Failure of the Strengthened Specimen

This failure mode was not observed during the previous study at University of Waterloo (McCarthy 2005), which was conducted on full length unstrengthened cross-arm members from Gulfport structures. In the full length experimental program, there was still considerable length of timber beyond the pinned end, which prevented this type of failure mode. Since the specimens that failed by splitting at the pinned end do not represent the actual field conditions, a pretensioned strap was applied to all of the specimens in Phases II and III of the experimental program to prevent the splitting of the member at the pinned end as shown in Figure 24. The application of this strap eliminated the splitting failure at the pinned end for both the control and strengthened specimens in Phases II and III.

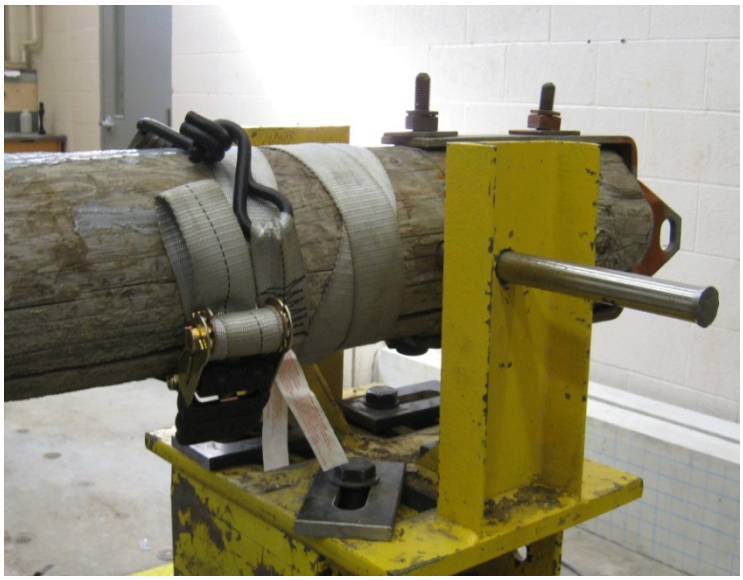

Figure 24: Pretensioned Strap

4.1.3 Effect of Moisture Content

The moisture content of wood members has a direct influence on its strength (Ho 2005). Therefore for the specimens to be comparable, they should have similar moisture contents. In order to have consistent moisture contents, all specimens were kept indoors for a period of 4 to 6 weeks prior to wrapping and then 2 weeks after wrapping for the strengthened specimens. The moisture content of all control samples was taken after testing their strength. The moisture content test for strengthened samples was not obtained due to the presence of the wrap in the proximity of the failure point.

The moisture contents were approximately 15% for samples C2 and C3, but the moisture content of sample C1 was approximately 19%. The difference in moisture content can be explained by the general conditions of each specimen. Specimen C1 had many large and deep cracks and thus water has had access to reach the core of the member. Sample S2 was cut from the same pole as C1, so it was expected to have similar moisture content.

Samples C1 and S2 had the lowest strengths within the control and strengthened categories, respectively. Interestingly, they were both cut from the same cross-arm which had approximately 27% higher moisture content than the other samples. The strength of wood and its modulus of elasticity both increase as its moisture content decreases (Ho 2005). Also, the presence of wide and deep cracks on this specific cross-arm had provided for the moisture to reach the core of the section and therefore the possibility of deterioration at the core of this sample was much higher than other samples. Visual inspection of the cross-sections of the cross-arms confirmed the presence of wood deterioration in the middle core of that particular pole. The deterioration was not continuous, but it was present as local deterioration in the core of member at a number of cross-sections along the length of the pole. The combined effect of the higher moisture content and presence of local deterioration in the core of the member most likely produced the lower strength results for samples C1 and S2.

4.1.4 Relationship Between Flexural Stiffness and Failure Load

The flexural stiffness of the specimens was computed through the analysis of the load versus deflection behaviour of the member. The control specimens exhibited a very linear load-deflection relationship up to failure, while the strengthened specimens experienced more ductile behaviour as the applied load reached the failure load of the specimen. Figure 25 illustrates the typical differences in load-deflection behaviour between the strengthened and the control samples.

Instead of analyzing the stiffness of the member in terms of its EI, the effective E was analyzed in order to take into account the variation of the moments of inertia for the different samples. Figure 26 illustrates the correlation between the effective Modulus of Elasticity (E) and the failure load of all six specimens. As shown in this figure, there is no correlation for the control specimens, while a strong correlation is present for the strengthened specimens with a R^2 value of approximately 0.91.

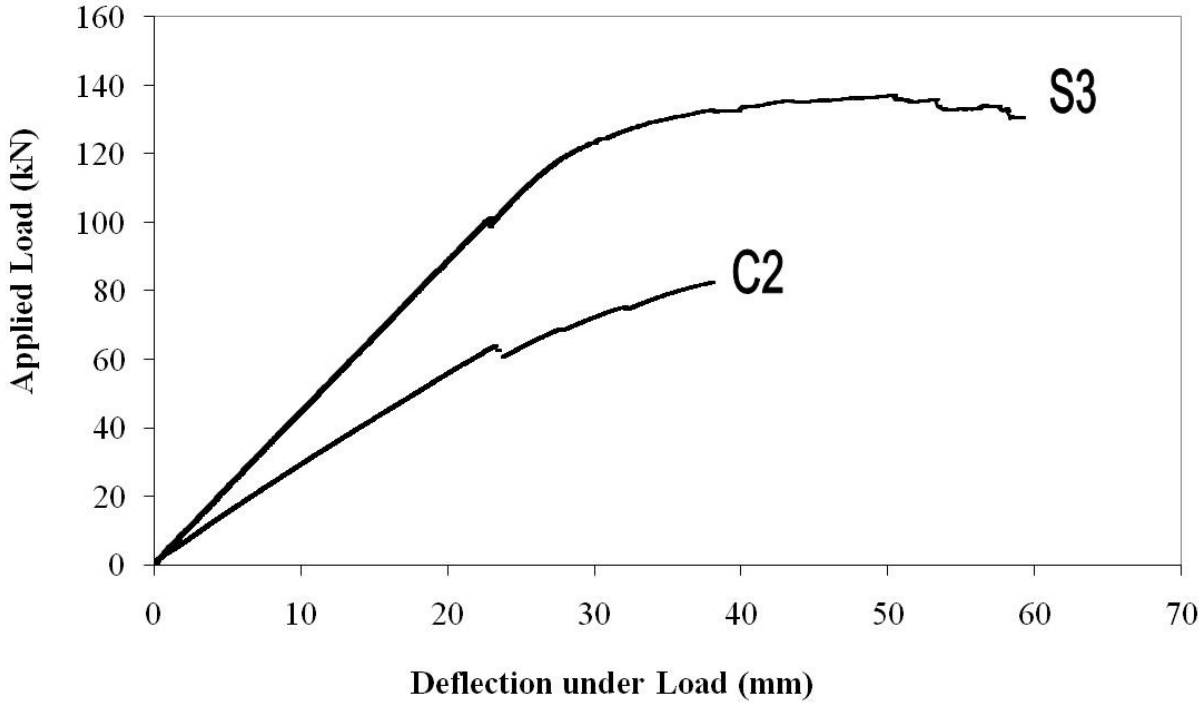

Figure 25: Typical Load-Deflection Behaviour (Strengthened and Control Specimens)

Figure 27 demonstrates the correlation between the bending stress and the effective Modulus of Elasticity (E) of all specimens. Again, there does not seem to be any correlation for the control specimens, while there is a positive correlation for the strengthened specimens with R^2 value of 0.61. The positive correlation indicates that as the effective E is increased, the failure stress and thus the strength of the specimen increase. The lack of correlation in the control specimens could be related to the effect of knots, cracks, and inconsistencies of the quality of wood in general. The effect of these inconsistencies is minimized in the strengthened specimens, since the failure load appears to be governed by the quality of the timber at the loading point and does not depend on the general quality of the member including knots and cracks.

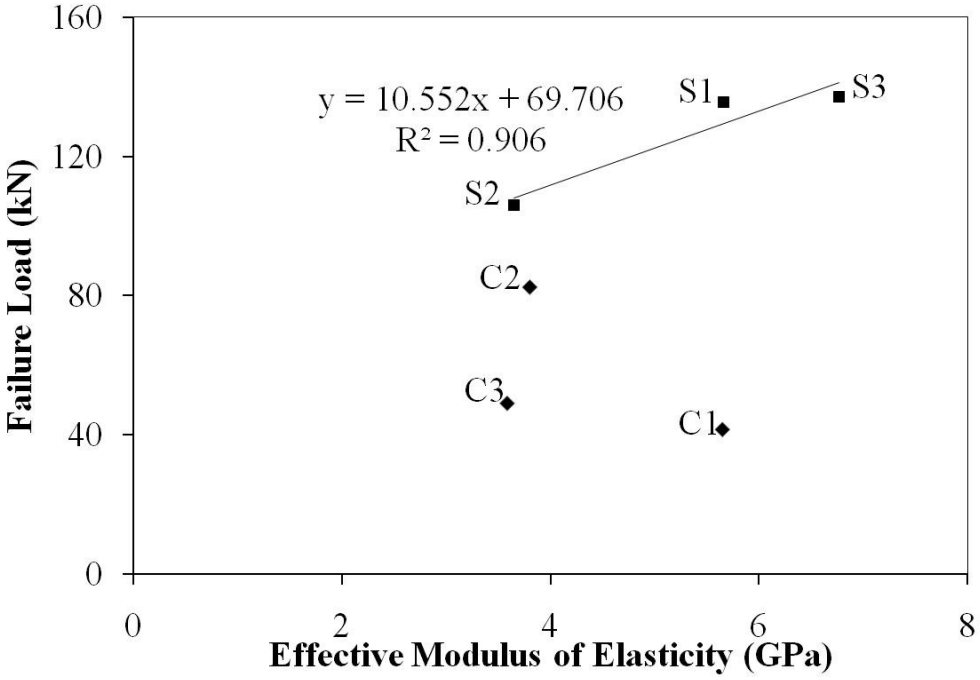

Figure 26: Correlation between Failure Load and Effective E

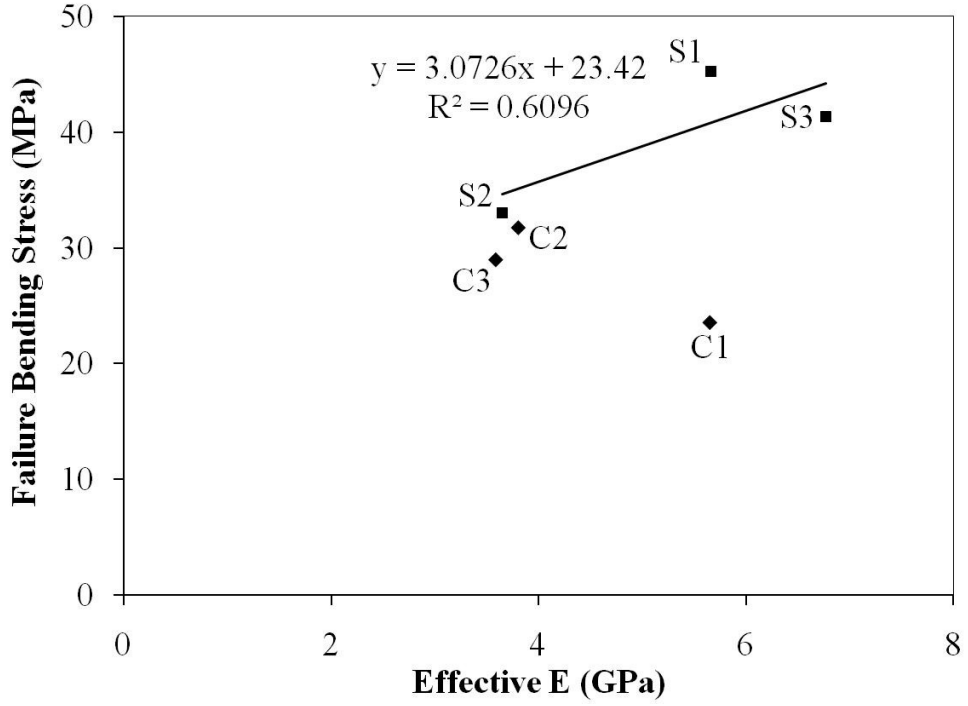

Figure 27: Correlation between Bending Stress and Effective E

4.1.5 Effect of Wrapping on Strength

The average failure loads for the strengthened specimens was approximately 118% higher than the average failure loads for the control specimens. Although the increase in the failure loads is very clear, the maximum bending stresses provide a more appropriate comparison tool since in this case the cross-section (diameter) of the members varied significantly. The average maximum bending stresses for the strengthened specimens was approximately 42% higher than the average bending stresses for the control specimens.

The increase in the maximum bending stresses was attributed to the presence of the GFRP wrap. Since the GFRP fibres were not oriented in the direction of the maximum bending stresses, the increase in strength was attributed to the shear strength and the confinement provided by the wrap. The confinement was assumed to increase the shear strength of the cross-arm, and prevent longitudinal cracking and splitting of the wood. This confinement also eliminated the combined shear-flexure failure and forced all strengthened samples to fail under pure flexure failure mode. Therefore, the variation in the strength of samples was only due to the variation in the quality of the wood at the loading point and was not related to the presence of knots, cracks, and other inconsistencies in the overall conditions of the member. Therefore, the strengthened samples had higher strengths as well as lower variation in comparison to the control specimens.

Although further data were required to provide a more accurate estimate for the expected increase in strength due to this strengthening system, the results of Phase I of the experimental program demonstrated the feasibility and potential of using this strengthening system for the proposed application.

4.1.6 Effect of Wrapping on Stiffness

Specimens S1 and S2 were initially loaded to approximately 10% of their estimated failure load to determine their initial stiffness prior to strengthening. Specimen S1 had a very solid

cross section with a minimal number of short length cracks and no signs of any longitudinal shear cracks along its length. Specimen S2 was severely cracked in the longitudinal direction at several locations around the circumference of the member. The surface cracks in specimen S2 reached the centre of the cross-section at different locations. The effective Modulus of Elasticity (E) of specimens S1 and S2 experienced an increase of 7% and 17%, respectively, as a result of the strengthening system. The effective Modulus of Elasticity was used as an indication of the stiffness of the member. Therefore, it was concluded that the strengthening mechanism had a greater impact on the stiffness of the deteriorated specimens in comparison to the specimens that were in better initial condition.

4.2 Phase II: Parametric Optimization

Phase I of the experimental program determined the proposed strengthening system can potentially increase the strength of the specimens by approximately 42%, which was deemed sufficient for the load carrying requirements of the Gulfport structures. Phase II of the experimental program was designed to investigate the effect of different variables that were involved in the strengthening system. The greater objective of this phase of the experimental program was to achieve the optimum configuration for the parameters that were involved in order to minimize cost, maximize practicality, and increase the efficiency of the strengthening system as much as possible.

As explained in the previous chapter, Taguchi Methods were used to design the experimental program of Phase II. The variables that were investigated in this phase of the experimental program are summarized in Table 16. The first column refers to the level of each factor, while the other four columns represent the factors that were investigated in this experimental design. For example, level 1 of deterioration (Factor D) refers to the minor deterioration, while level 2 refers to heavy deterioration. The description of each variable is given in the experimental design chapter of this thesis; however, it is important to note that Deterioration, Factor D, refers to the extent of surface deterioration and does not directly relate to the

internal deterioration of the samples. The internal deterioration was not studied as part of the Taguchi Design experiments, as sufficient numbers of specimens with internal rot were not available.

Table 16: Phase II Parameters and Levels

Level	Deterioration (D)	Width of Wrap (A)	Filler Material (B)	Sanding (C)
1	Minor	1.2 m	None	No
2	Heavy	0.6 m	Anchorfix-3	Yes

4.2.1 ANOVA Analysis

An orthogonal array with 8 experiments (OA8) was chosen for the experimental program of Phase II. The experimental results of all 8 specimens are presented in Table 17. All four response variables that are analyzed separately using ANOVA are presented in this table, including: Effective E, Maximum Load, Maximum Deflection and Bending Stress.

Table 17: Phase II Orthogonal Array and Experimental Results

Sample	Diameter (mm)	Effective E (GPa)	Max. Load (kN)	Max. Def. (mm)	Bending Stress (MPa)	Failure Mode
S22	267	2.65	97	70	36.1	Flexure-Tension
S32	283	3.69	106	43	33.0	Flexure-Tension
S42	274	3.68	92	43	31.6	Flexure-Tension
S82	258	5.56	124	49	51.3	Flexure-Tension
S12	280	3.37	93	43	29.8	Flexure-Tension
S52	269	5.49	119	40	43.0	Flexure-Tension
S62	269	4.95	112	42	40.6	Flexure-Tension
S72	240	7.53	127	50	50.7	Flexure-Tension

The following analyses are based on the maximum load as the response variable. All of the equations presented in this chapter have been taken from Roy (2001). These equations are consistent through all references. The first step in the ANOVA analysis is to determine the sum of squares for each column in the experimental program. The general formula for calculating the sum of squares of column A with k levels is:

$$\textbf{Equation 2:} \quad SS_A = \left[\sum_{i=1}^{k_A} \frac{A_i^2}{n_{A_i}}\right] - \frac{T^2}{N}$$

In Equation 2, A_1 refers to the sum of all the values of a given response variable that include the factor A at level 1, T is the sum of all response values, N is the total number of specimens, and n_{A_i} is the number of specimens under level i of variable A. For example, in the above example, A_1 is equal to the sum of the maximum loads of samples S022, S021, S012, and S052, which is equal to 415 kN. In this case the entire experimental program consisted of two level factors; therefore Equation 2 reduces to Equation 3.

$$\textbf{Equation 3:} \quad SS_A = \frac{(A_1 - A_2)^2}{N}$$

In the above equation A_2 refers to the sum of all the values of a given response variable that include the factor A at level 2. The degrees of freedom (DOF) associated with each column play a significant role in the ANOVA analysis. The degree of freedom for column A is given in Equation 4 and the degree of freedom for a column carrying the interaction of A×B is given in Equation 5.

$$\textbf{Equation 4:} \quad V_A = k_A - 1$$

$$\textbf{Equation 5:} \quad V_{A\times B} = (V_A) \times (V_B)$$

In the above equations $\boldsymbol{V_A}$ refers to the variance associated with Factor A. Table 18 summarizes the ANOVA calculations of Phase II experimental program for maximum load as the response variable. In this table, variance is equal to the sum of squares divided by the corresponding degrees of freedom. As explained earlier, the variance values can be used to determine the most influential factor for a given response variable. The significantly higher value of the variance of the factor B, the use of filler material, means that this factor was most responsible for the variation of the response values, which corresponds to the failure loads in this case. In other words, factor B was the most influential factor in this experimental program. The two interactions that were investigated both had variance values below or close to the variance of the error and therefore were deemed statistically insignificant and were summed up with the error as "pooled error".

Table 18: ANOVA Calculations for Maximum Load

Column	Factor	SS	D.O.F	Variance
2	A	197.0	1	197.0
4	B	854.9	1	854.9
7	C	146.0	1	146.0
1	D	119.0	1	119.0
3	D&A	29.7	1	29.7
5	D&B	0.1	1	0.1
6	error	22.1	1	22.1
Total		1368.9	7	

Table 19 summarizes the modified ANOVA calculations with the pooled error. The F-Test value is also presented in this table, along with percent contribution of each factor towards total variation in the samples. As with the variance, the higher values of F and P represent a stronger contribution and therefore represent a more significant factor.

Table 19: Modified ANOVA for Maximum Load

Column	Factor	SS	D.O.F.	Variance	F - Test	P (%)
2	A	197.0	1	197.0	11.39	14.4
4	B	854.9	1	854.9	49.42	62.5
7	C	146.0	1	146.0	8.44	10.7
1	D	119.0	1	119.0	6.88	8.7
6	Error Pooled	51.9	3	17.3	1.00	1.3
Total		1368.9	7			

The F-test values for the given degrees of freedom and confidence levels of 99%, 95%, and 90% are 34.116, 10.128, and 5.538 respectively (Belavendram 1995). Therefore, it was concluded with a 99% confidence level that factor B was statistically significant. The confidence level for factor A was 95% and for factors C and D the confidence level for statistical significance was 90%. This information is valuable, but still does not specify the optimal level of each variable.

Taguchi categorizes all experiments into three groups based on their desirable outcome: higher the better (HB), nominal the better (NB), and lower the better (LB). He has used these categories to formulate loss functions, which is beyond the scope of this thesis. This experimental program had a higher the better response variable as higher failure loads were desirable. Depending on the category of the response variable, Taguchi recommends a number of ways for determining the optimal level of each factor that would yield the most efficient solution. For the purposes of this research, the graphical approach was the most suitable technique for choosing the optimum levels. Figure 28 shows the factors and the mean value of the response variable in terms of the failure load, at different levels of the factors investigated in this phase of the experimental program.

Since this experimental program had a “higher the better” response variable, the levels of each factor which correspond to a higher mean value of the response variable were chosen.

Therefore, the optimal design was A_2-B_2-C_1-D_2, which would translate into using 0.6 m wide GFRP wrapped around a filled in, but non sanded, surface. It also suggested that higher surface deterioration increased the failure load. Higher deterioration could be beneficial in two ways: the presence of high volume of filler material and by providing a rougher surface for better bond. The filler material, Sika AnchorFix3, was a very strong binder and by eliminating the gaps in the cracks prevented the cracks to grow during loading. This filler material also provided for solid surface for the application of the wrap, as the samples that were not crack-filled had air pockets under the wrap that may have weakened the bond between the GFRP and the wood.

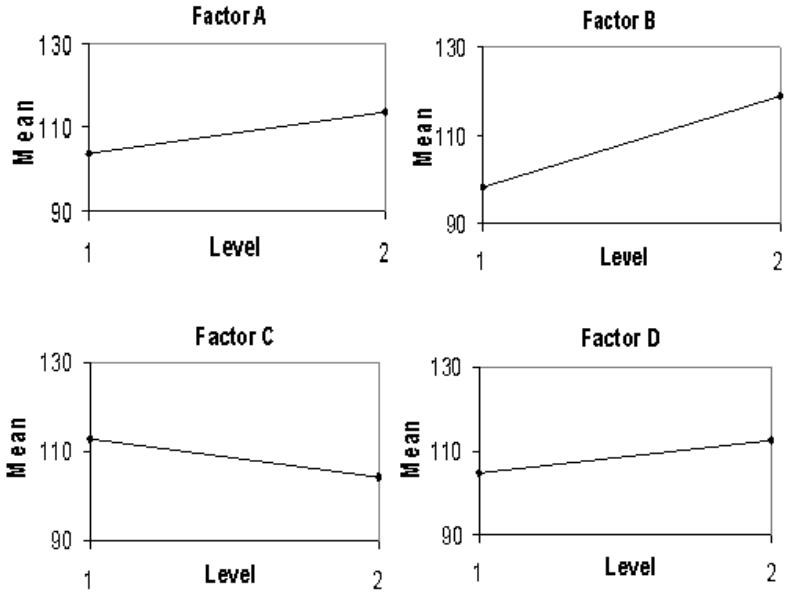

Figure 28: Graphical Approach for Optimal Level Selection

The optimal levels for factors C and D were consistent with results of the research of Lyons and Ahmad (2005) who concluded that FRP wrap bonds better to rougher surfaces (Ahmed and Lyons 2005). Specimens with higher surface deterioration (D2) and non-sanded surface (C1) provide a rougher surface, and therefore better bond was achieved. It is important to note that Lyons and Ahmad also concluded that the effect of the rough surface, although positive, was not very significant. This conclusion was also verified by noting the effects of

variables C and D are not statistically significant based on 95% confidence level, which is usually used for most experimental programs.

The optimum level of factor A, the width of wrap, suggests the use of a shorter width of wrap of 0.6 m instead of 1.2 m. This conclusion was statistically significant with a confidence level of 95% and could not be ignored or related to error of experimentation. This observation was also consisted with the results of Phase I of the experimental program. In the previous phase the sample with the shorter width of wrap supported equal or even higher loads than the wrapped specimens with full width of wrap. The sample wrapped with the shorter wraps, sample S1, failed due to splitting at the end, which was avoided in Phase II by using a pre-tensioned strap around the circumference of the member at the pinned end. In other words, if the splitting at the end was avoided in the Phase I and considering the load-deflection behaviour of samples S1, S2, and S3 in that phase, sample S1 would likely fail at a higher load than all other strengthened samples.

All of the control samples that were tested as part of the different phases of the experimental program of this thesis failed under the loading point by combined flexure and shear, except for those that failed by splitting at the pinned end during Phase I. However, all of the wrapped specimens, with the exception of sample S2 that failed due to splitting at the pinned end, failed due to pure flexure at the loading point. Analysis of the failure modes showed that the switch from combined shear and flexure failure mode for the control specimens to pure flexure failure of the strengthened specimens was a direct result of the strengthening system. This observation suggested that the confinement aspect of the GFRP wrap was working close to the loading point, therefore going from a width of 0.6 m to 1.2 m was not expected to have a significant further improvement.

The higher performance of the specimens wrapped with the shorter width of GFRP wrap is illustrated in Figure 29. The figure at the top is representative of the behaviour of the two groups of strengthened samples on average. The bottom figure is not exactly consistent with

the top figure, as it includes some scatter in the data, and it is included only for completeness. The specimens with shorter width of wrap failed at higher loads but on average had lower deflections in comparison to the specimens wrapped with full width of the wrap. Also, this figure suggests that the specimens with half width of wrap have higher stiffness than the samples with the full width of wrap. The stiffness criterion is analyzed as a separate ANOVA analysis later in this section to further investigate the better performance of the shorter width of wrap.

The optimal level of factor A was very beneficial to the practical aspects of this strengthening solution as it cuts the cost of material by 50%, while also providing a much easier application procedure, since working with the smaller sized wrap was significantly easier than the longer wrap. The simpler application is very valuable for field application.

Although the analysis of the failure load as a response variable was of a great interest, it is more accurate to analyze the maximum bending stress as a response variable since the analysis of the bending stress accounts for the varying diameter size of the specimens. Table 20 summarizes the ANOVA calculations for Phase II based on maximum bending stresses.

Table 20: ANOVA Calculations for Maximum Stress

Column	Factor	SS	D.O.F	Variance
2	A	137.5	1	137.5
4	B	208.3	1	208.3
7	C	89.9	1	89.9
1	D	15.5	1	15.5
3	D&A	4.0	1	4.0
5	D&B	7.4	1	7.4
336	error	42.9	1	42.9
Total		506	7	

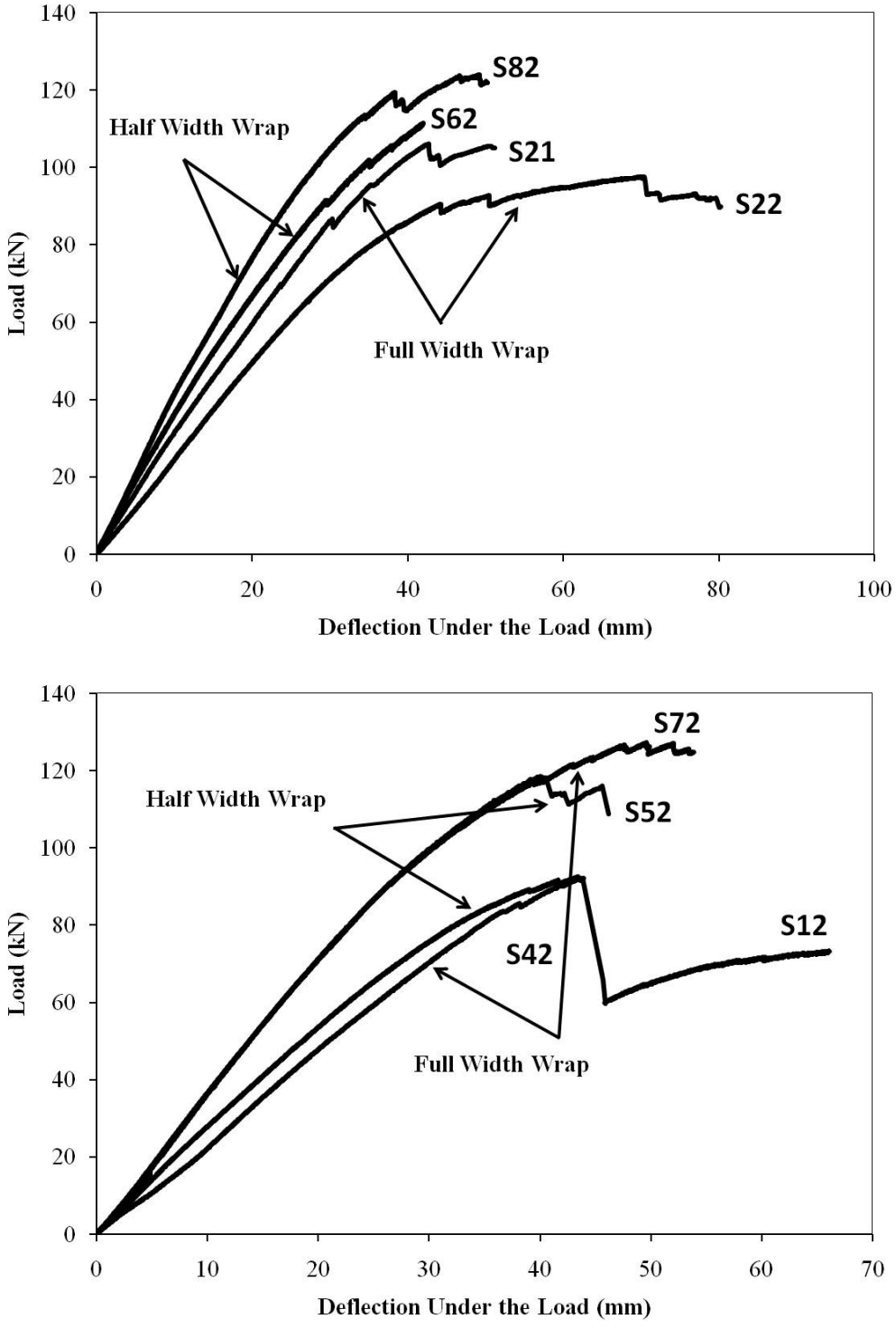

Figure 29: Load-Deflection Relationship for Selected Phase II Specimens

Table 21 summarizes the modified ANOVA results for Phase II of the experimental program based on the maximum stress as the response variable. As can be seen from this table the percent contribution of the factors are different than those obtained from the previous round of ANOVA calculations based on the maximum load as the response variable, however, the relative effect of factors remains the same, with Factor B having the greatest effect (41.2%) followed by Factors A, C, and D respectively.

The third response variable that was analysed using ANOVA was the deflection at the maximum load. Table 22 summarizes the ANOVA results for this response variable. The effect of the error of the experiment was much greater than the effect of any other factor. This result meant that none of the factors could be deemed statistically significant, regardless of the confidence interval that was chosen. In other words, none of the factors or interactions listed in Table 22 could be held responsible for the variation of the deflection data. In this experiment, "error" refers to the combination of the error of the experiment and the effect of all other variables that were potentially present and not included in the experimental design.

Table 21: Modified ANOVA for Maximum Stress

Column	Factor	SS	D.O.F.	Variance	F - Test	P (%)
2	A	137.5	1	137.5	7.87	27.2
4	B	208.3	1	208.3	11.92	41.2
7	C	89.9	1	89.9	5.15	17.8
1	D	15.5	1	15.5	0.89	3.1
6	Error Pooled	69.9	4	17.5	1.00	3.5
Total		505.5	7	0		

Table 22: ANOVA Calculations for Deflection

Column	Factor	SS	Dof	Variance
2	A	18.9	1	18.9
4	B	36.7	1	36.7
7	C	61.5	1	61.5
1	D	111.8	1	111.8
3	D&A	101.0	1	101.0
5	D&B	81.6	1	81.6
6	error	244.8	1	244.8
Total		656.3	7	

The analysis of the maximum load as the response variable did not yield a high error factor as the main factors controlling the maximum load were included in the experimental program. However, none of these factors were responsible for the variation of the deflection response, and hence the error of the experiment was very high for that particular response. Other factors such as the age of the timber, moisture content, and internal deterioration were not studied but could potentially be responsible for the variation in the deflection response. The incorporation of the error column can ensure the validity of the results as seen in the above example. This verification is often missing in other types of experimental design, or even Taguchi designs that do not leave extra degrees of freedom for the error. Having a low error indicates that most of the factors that were responsible for the variation within the population of specimens were accounted for in the other columns of the experimental design.

A third ANOVA analysis was conducted based on the effective Modulus of Elasticity as the response variable. The purpose of this analysis was to investigate the factors that control the effective Modulus of Elasticity and therefore the stiffness of the member. This information was needed to help explain the results of the first ANOVA analysis with respect to the specimens wrapped shorter width of wrap outperforming the ones wrapped with the longer width of wrap. The effective Modulus of Elasticity was calculated using Equation 1 (section

4.1). The ANOVA calculations for the effective Modulus of Elasticity as the response variable are summarized in Table 23.

Table 23: ANOVA Calculations for Effective E

Column	Factor	SS	Dof	Variance
2	A	5.21	1	5.21
4	B	6.98	1	6.98
7	C	0.01	1	0.01
1	D	4.34	1	4.34
3	D&A	0.04	1	0.04
5	D&B	0.37	1	0.37
6	error	0.27	1	0.27
Total			7	

The ANOVA results for the effective Modulus of Elasticity produced interesting results and were accompanied with a very low indication of error. The effect of sanding and the interactions were insignificant, however, Factors A, B, and D had very high variances. The modified ANOVA is presented in Table 24. The ANOVA analysis indicated that Factors B (Filler Material), A (Width of Wrap), and D (Surface Deterioration) were responsible for 40%, 30% and 25% of the variations in the results, respectively. According to the F-test values, Factors B, A, and D are statistically significant with a confidence level of 99%, 95%, and 95%, respectively. Further analysis of ANOVA results indicated that shorter width of wrap, application of Sika AnchorFix3 filler, and heavy surface deterioration would result in the highest effective Modulus of Elasticity for the specimens. From the limited data of this experimental program, the reason for the samples wrapped with the shorter width of wrap having higher Effective E values than those wrapped with the full width of the wrap was not evident, and further research is required to investigate the reasons for this behaviour. This result is consistent with the load-deflection behaviour of the strengthened specimens

illustrated in Figure 29. The higher slope of the load-deflection behaviour of the specimens wrapped with the shorter width of GFRP wrap indicated that they had higher stiffness.

Table 24: Modified ANOVA for Effective E

Column	Factor	SS	D.O.F.	Variance	F - Test	P (%)
2	A	5.214	1	5.21	30.22	30.3
4	B	6.983	1	6.98	40.48	40.5
1	D	4.341	1	4.34	25.17	25.2
6	Error Pooled	0.690	4	0.17	1.00	1.0
Total		1368.9	7			

4.2.2 Estimating the Mean and Confidence Interval

One of the main advantages of using a statistically designed experimental program is the ability to estimate the average response variable for any given configuration of the factors. More specifically, when the experimental program is designed using the Taguchi Methods, Analysis of Variation (ANOVA) enables the researcher to estimate the average of the optimal configuration with a known confidence level. From the previous discussions in this paper, the researcher is able to choose what levels of the factors involved would yield the optimal outcome, however being able to estimate the range of that optimal outcome with a known level of confidence is very useful in design applications.

The Equation 6 (Roy 2001) was used to calculate the estimated mean for the optimal configuration A_2, B_2, and C_1. Note that Factor D was a noise factor, by definition, since it could not be controlled or be assigned a specific level.

Equation 6: $\bar{\mu}_{A_2B_2C_1} = \overline{A_2} + \overline{B_2} + \overline{C_1} - 2\overline{T}$

In the above equation, the first three terms corresponding to the average response variable of the corresponding level of each factor, and T represents the average of all responses.

The estimate of the mean is only a point estimate based on average of results obtained from the experiment. Therefore, there is a 0.5 probability of true average being greater than or less than the estimated mean. Therefore, specifying a range in which the true mean would be expected at a given confidence level is very desirable. This could be achieved by the use of confidence intervals, given by Equation 7 (Roy 2001).

Equation 7: $$CI = \sqrt{\frac{F_{\alpha,\upsilon 1,\upsilon 2} \times V_e}{n}}$$

In the above equation, CI is the confidence interval, α is the risk, υ_1 is the degree of freedom for mean (equals to 1), υ_2 is the degree of freedom for error (equals to 3 in this experiment), V_e is the variance of error, and $F_{\alpha\upsilon 1\upsilon 2}$ is the F-ratio (obtained from statistics tables).

Using the above equations with a confidence level of 95%, the estimated mean for the failure load of the strengthened specimens using the optimal configuration (A_2-B_2-C_1) was 128 kN with the following confidence interval: 115 kN < True Mean < 141 kN. Also, using a confidence level of 95%, the estimated mean for the maximum stress of the strengthened specimens using the optimal configuration (A_2-B_2-C_1) was 52 MPa with the following confidence interval: 38.7 MPa < True Mean < 65.31 MPa.

It was concluded that using statistical tools to design an experimental program and to analyze the results of that program can provide very valuable information that was otherwise not possible to obtain. Providing estimated mean with known confidence level and a specific confidence interval was not usually stated in Civil Engineering related research programs due to the lack of systematic experimental design and data analysis tools. However, these methods have been extensively used in mechanical and computer related research and have provided invaluable information to researchers in these fields (Bendell et al. 1989). With the

use of these statistical tools, research programs will be able to support their arguments and have a more influential impact on their specific field of research.

4.3 Phase III: Confirmation Testing

Phase III of the experimental program was designed based on the findings of Phase II, outlined above. Confirmation testing is in fact the last step in a complete Taguchi Design experimental program. The purpose of the confirmation testing in Taguchi Design, in addition to confirming the results of ANOVA, is to narrow the confidence interval that was suggested using the ANOVA calculations. The confidence interval can be narrowed when more samples are added to the population. For example, increasing the number of specimens by a factor of four would narrow the confidence interval by 50%. The confidence interval that was calculated in the previous section was acceptable for the purposes of this research project, as the minimum value of that range was well above the design requirements of the Gulfport Structures. However, the confirmation testing was still performed to confirm the ANOVA calculations to show that the statistical principles applied in thesis are applicable to Civil Engineering applications by confirming ANOVA results with experimental results.

Three samples were prepared for the confirmation testing using the same procedures explained earlier in this thesis. The optimal configuration that was obtained from Phase II was applied to all specimens, as the main objective of this phase of testing was to confirm the expected results of the previously recommended optimal design.

Due to the lack of inventory on cross-arm samples, specimens with smaller diameters had to be used for the Phase III of the experimental program. These specimens were cut from the same original cross-arms that other specimens were obtained, however, they were cut from other sections of the cross-arms and therefore had smaller diameters. Due to the significant difference in the diameters, the results were not comparable in terms of maximum load, but

since the same wood was being tested, the results were compared on the basis of maximum stress.

Table 25 summarizes the results for the specimens tested in Phase III of the testing program. All of the samples were within the range that was estimated using 95% confidence interval, and the data were spread over a much narrower range than the estimated confidence interval. Therefore, it was concluded that the 95% confidence interval was accurate. The number of samples tested in this phase was not sufficient to reduce the confidence interval significantly, however the results demonstrated that ANOVA calculations and estimation of the mean and confidence interval were accurate and that the actual confidence interval for 95% confidence could be reduced by increasing the number of specimens tested.

Table 25: Phase III Confirmation Testing Results

Sample	Diameter (mm)	Deflection (mm)	Max. Load (kN)	Stress (MPa)	Failure Mode
S031	178	41.16	50.92	64.1	Flexure-Tension
S032	194	49.68	66.86	64.9	Flexure-Tension
S034	182	45.07	50.63	59.6	Flexure-Tension

4.4 Material Testing

The cross-arms were tested for two types of material testing: shear-parallel-to-grain test and compression-parallel-to-grain test. The results of these tests are summarized in this section. The moisture contents for each tests are also presented, as moisture content has a significant role in the material properties of wood.

4.4.1 Shear Parallel to Grain Test Results

The shear-parallel-to-grain test was conducted in accordance with the Standard Test Methods for Small Clear Specimens (ASTM: D143-94 [Reapproved 2007]). The samples were tested to failure and then the moisture content test was conducted on the sample. Total of 29 samples were tested for Shear-Parallel-to-Grain and the results are summarized in Table 26.

Table 26: Shear-Parallel-to-Grain Test Results

	M.C. (%)	Shear Stress (MPa)	Int. LVDT (mm)
Average	8.58	3.15	1.52
St. Dev	0.92	0.48	0.92
Min	6.62	2.42	0.77
Max	10.38	4.17	5.45

The results were relatively consistent with an average of 3.15 MPa and standard deviation of 0.48 MPa. The last column in Table 26 represented the deflection of the specimen at failure, which was recorded by the internal LVDT in the actuator. Figure 30 shows a histogram of the distribution of the shear strength of the samples.

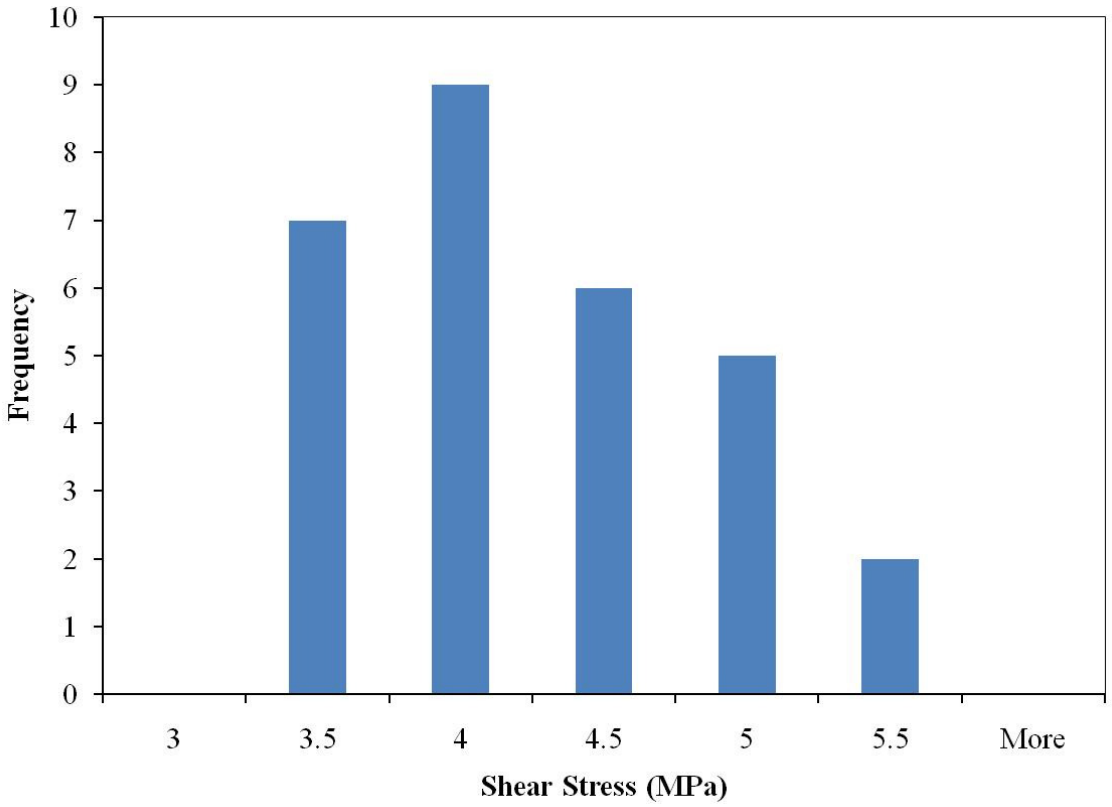

Figure 30: Histogram for Shear Strength

The Forest Service in United States publishes various statistical data with respect to forestry and timber products that are grown in United States or grown in other countries and imported to United States. This service was established in 1905 and is an agency of the United States Department of Agriculture. The mechanical properties of Canadian grown Jack Pine are summarized in Table 27. The reported values for the shear-parallel-to-grain test in Table 27 are almost two times higher than those obtained from the experimental results. The significant difference between the two values suggests that the material properties of the Gulfport cross-arms have greatly depreciated during the last thirty years. The deterioration of the material properties could be due to internal rot of the members, use of creosote treatment, or aging of the structure.

Table 27: Mechanical Properties of Canadian Grown Jack Pine (U.S. Department. of Agriculture)

Moisture Content	Specific Gravity	Modulus of Elasticity	Compression parallel to grain	Compression perpendicular to grain	Shear parallel to grain
		(MPa)	(kPa)	(kPa)	(kPa)
Green	0.42	8100	20300	2300	5600
12%		10200	40500	5700	8200

Figure 31 illustrates the relationship between the shear stress and the moisture content. The trend line suggests a weak positive correlation between the two variables. Samples at higher moisture contents would be needed to confirm and explain this correlation. Figure 32 shows one of the failed samples. All of the specimens failed in the predefined shear plane as shown in this figure. The figure to the left shows a side view of the failed sample and the figure on the right is a front view of the same sample. The wedge-like texture of the failed specimen was similar for all specimens.

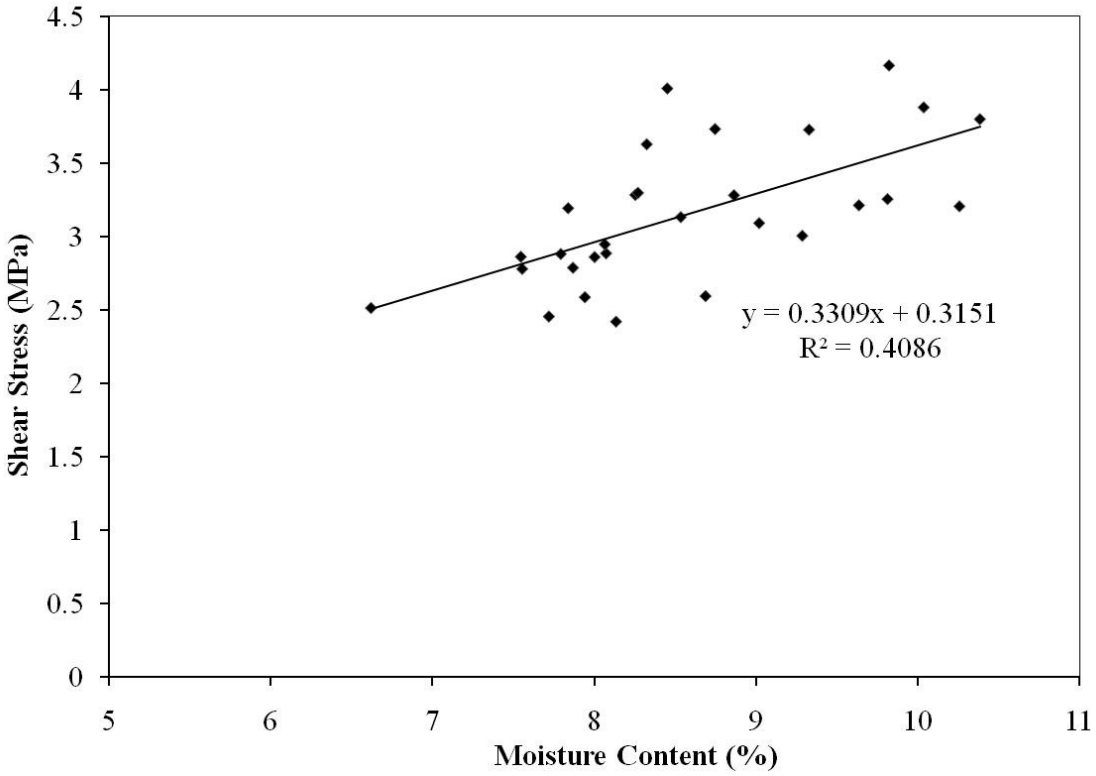

Figure 31: Shear Stress vs. Moisture Content

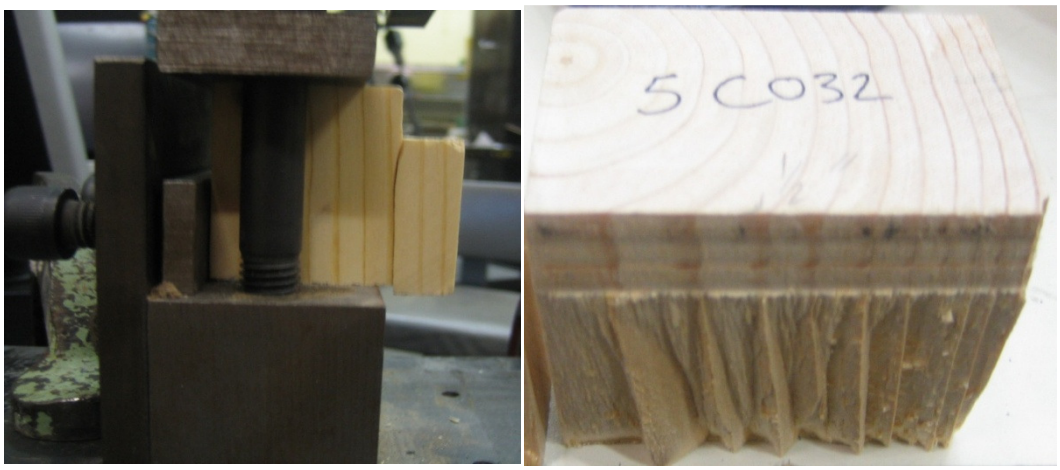

Figure 32: Shear-Parallel-to-Grain Test Sample

4.4.2 Compression Parallel to Grain Test Results

The compression-parallel-to-grain test was conducted in accordance with the Standard Test Methods for Small Clear Specimens of Timber (ASTM: D143-94 [Reapproved 2007]). A total of 12 samples of 5.08 by 5.08 by 20.32 cm [2 by 2 by 8 in.] were tested for compression-parallel-to-grain and there were all tested for moisture content after the test. The samples were tested using a 55 kip capacity MTS frame, with the load being applied continuously at a rate of 0.6 mm/min, as per ASTM specifications.

The results and the statistical data for the compression-parallel-to-grain tests are summarized in Table 28. These results can be compared with those summarized in Table 27. In this case the experimental results are much more comparable to the data posted by the Forest Service. The last column in Table 28 represents the deflection of the specimen at failure, which was recorded by the internal LVDT in the actuator.

Table 28: Compression-Parallel-to-Grain Test Results

	M.C. (%)	Stress (MPa)	Int. LVDT (mm)
Average	8.87	35.06	5.93
St. Dev	1.50	7.94	0.88
Min	7.44	24.19	3.79
Max	12.12	49.68	7.11

Figure 33 presents the relationship between the moisture content and failure load of the specimens for the compression-parallel-to-grain tests. Although the R-square value is fairly low, a similar trend to the shear-parallel-to-grain test seems to be present. Out of the 12 samples that were tested, six failed in crushing, three failed in splitting, two failed in end rolling, and finally one sample failed in shearing. The difference in the failure modes was mainly due to the presence of knots, and in the case of splitting failures, due to the presence

of cracks. Unfortunately, due to the thick layer of creosote on the poles and also the deteriorated nature of the cross-arms, only a limited number of clear and un-cracked samples with no creosote were obtained. Due to the health risks associated with creosote and lack of adequate ventilation in the laboratory, material testing was only conducted on the pieces that did not have any creosote. The areas covered by creosote also had many splits, which would not allow for obtaining clear samples. The sample preparation was conducted outside of the lab to obtain the clear samples.

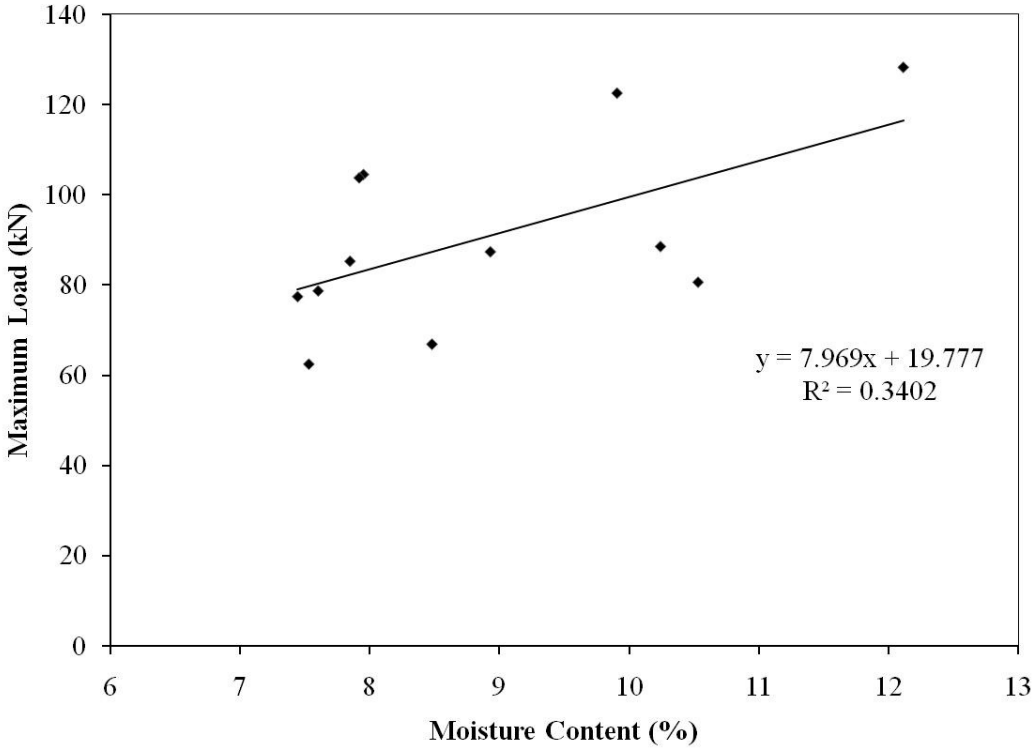

Figure 33: Maximum Compression Load vs. Moisture Content

5 Evaluation of the Strengthening System

In this chapter, the end of life (EOL) modulus of rupture limit for the Gulfport structure is compared against the capacity of the strengthened specimens to evaluate the performance of the strengthening system. The failure mechanism of the strengthened specimens is also presented, along with a discussion of the local failures that were caused by the extremely high load levels of the strengthened samples. The analysis of the strain data is also presented in this chapter.

5.1 Gulfport Design Requirements

As reported in Chapter 2, the Canadian and American standards, CSA C22.3 No.1-01 and National Electrical Safety Code C2-1993, define the end of life (EOL) of a cross arm as the point when the pole has deteriorated to two thirds of its original strength (McCarthy 2005). Consequently, the EOL for Gulfport cross arms in terms of Modulus of Rupture is 30 MPa (approximately 4400 psi). Therefore, any specimen with a Modulus of Rupture greater than 30 MPa is considered adequate for the purposes of the Gulfport structures, based on the EOL stress limit.

Previous condition assessment research at University of Waterloo (McCarthy 2005) for Ontario Hydro, the owner of the Gulfport Structures in Ontario, have also used the EOL threshold of 30MPa as the minimum strength requirement for structures to remain in service.

5.2 Performance of Strengthened Specimens

The stressed based ANOVA analysis estimated the average Modulus of Rupture for the strengthened specimens to be 52 MPa, with a 95% confidence interval of: 38.7 MPa < True Mean < 65.31 MPa. The EOL threshold for these members is 30 MPa, therefore the mean strength of the strengthened specimens is 73% stronger than the specified EOL. The

minimum value of the 95% confidence interval is still greater than the EOL threshold, however it should be noted that this range is wide due to the limited number of specimens, and therefore the minimum value is considered to be extremely conservative. The confirmation samples (Phase III) ranged from 59.6 MPa to 64.9 MPa, which suggests that the confidence interval can be significantly reduced by testing more samples and that the true mean is much closer to the higher end of the initial confidence interval. It should be noted again that increasing the number of specimens by a factor of four, reduces the confidence interval by 50%.

It is very important to note that the control and strengthened samples were taken randomly from the same set of poles provided by Ontario Hydro. All of the provided poles were removed from service as they seemed inadequate for the requirements of Gulfport structures, using the current condition assessment techniques of Ontario Hydro. Two of the three control specimens failed the EOL threshold of 30 MPa, while all of the strengthened specimens exceeded this threshold, with no exception. Also, the strengthened specimens had an average Modulus of Rupture value that was more than 70% larger than of the EOL threshold. Therefore, the strengthening system was concluded to be very effective for the purposes of strengthening deteriorated cross arms of the Gulfport structure.

5.3 Flexural Failure of Strengthened Specimens

Analysis of the experimental data showed that the strengthened samples, in addition to having higher capacities, were more consistent in terms of maximum loads and maximum stresses. The reason for the consistency of the results was due to the increased consistency of the failure modes. The majority of the control samples failed by the combined shear-flexure failure mode. However, the depth and the length of the shear cracks varied between the samples, and therefore the capacity of the control specimens was more varied than that of the strengthened specimens. Initial conditions including existing cracks, knots, and moisture contents of the specimens were the major sources of variation in the data.

The failure loads and stresses of the strengthened specimens demonstrated much narrower ranges than those of the control specimens. The consistency of the strengthened samples was due to the failure mode of these specimens. The presence of the circumferential GFRP wrap eliminated the shear cracks that were developed below the loading point in the control specimens, and therefore the failure mode was forced to be a pure flexural failure near the load point. Since the failure was controlled by the capacity of the wood at that particular cross-section, which was more or less consistent between different poles as long as there was no indication of deterioration in the cross-section, the variability in the failure loads of the strengthened specimens were much lower than those of the control specimens. Figure 34 shows a typical pure flexural failure of the strengthened specimens.

Figure 34: Typical Flexural Failure for Strengthened Specimens

The strengthened samples in this experimental program were exposed to much higher loads than the expected design load for the cross-arms. The high loads for some specimens also caused other local failures, particularly at the loading piece and at the supports. Figure 35-A shows a crushing failure of timber and FRP under the loading piece. The crushed depth of timber reached 20 mm in some cases. The timber at the support locations also experienced crushing damage in some specimens. Figure 35-B shows the crushing of the filler material in the cracks under the load piece.

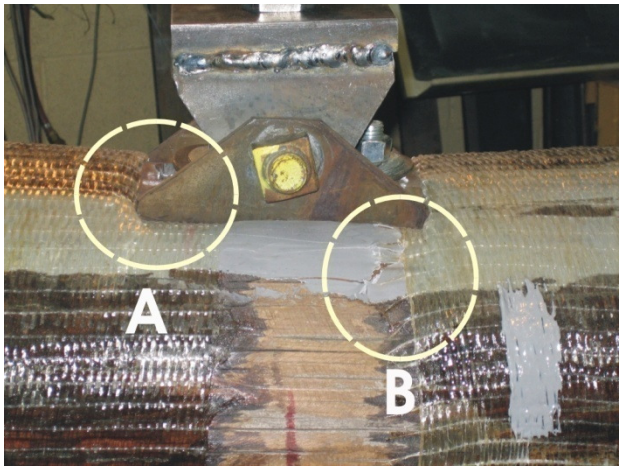

Figure 35: Local Crushing Failure under Loading Point

The bond between the GFRP and the timber proved to be very effective, particularly in Phases II and III of the experimental program, where the surface of the specimens were not sanded. However, one specimen in the Phase I of the experimental program demonstrated a local bond failure between the GFRP and timber, as shown in Figure 36. The surface of the sample shown in this figure was sanded using an electric sander. The length of the slip reached 15 mm at the maximum slip section, as identified with the white arrows in Figure 36. This local failure was only limited to this particular sample, and was most likely due to the smoothened surface of the timber.

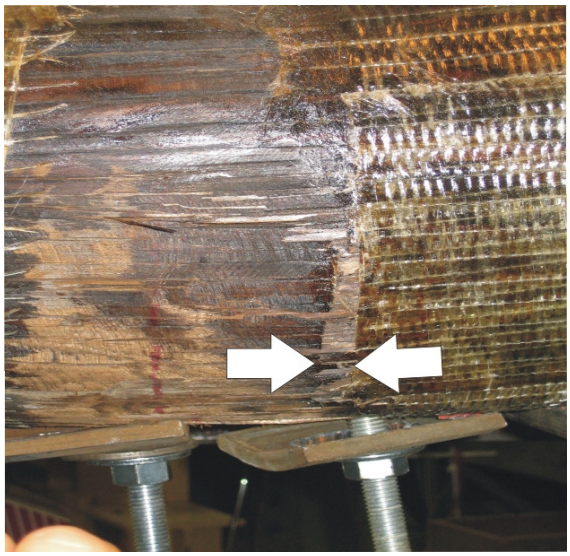

Figure 36: GFRP Slip on Wood Surface

The ultimate elongation of the cured laminated state of the GFRP wrap was 2.45%, according to SIKA Canada. The strain gauges installed circumferentially on the GFRP only measured a maximum elongation of 0.2% indicating that the wrap was well below the limiting rupture strain and that one layer of wrap was sufficient for the confinement purposes. However, the ultimate elongation of the cured laminated state of GFRP wrap perpendicular to the main direction of wrap was only 0.46%. This limit may have been reached in one of the specimens, resulting in a local failure of the matrix of the strengthening system, as shown in Figure 37. This sample was strengthened using full width of the wrap and the picture was taken from underneath the specimen. These failures were only present on the tension side of the specimens and were due to the large flexural tension strains developed in the member. The hook that was used to connect the strain potentiometer to the beam might have initiated the cracking at this area, and therefore LVDTs were used for all other specimens. Since this type of local failure only happened on one sample, no conclusions could be made with respect to the cause or the effect of this local failure. However, no effect on the strengthening system is expected as the main fibres were still intact and only the matrix of the strengthening system failed in this case.

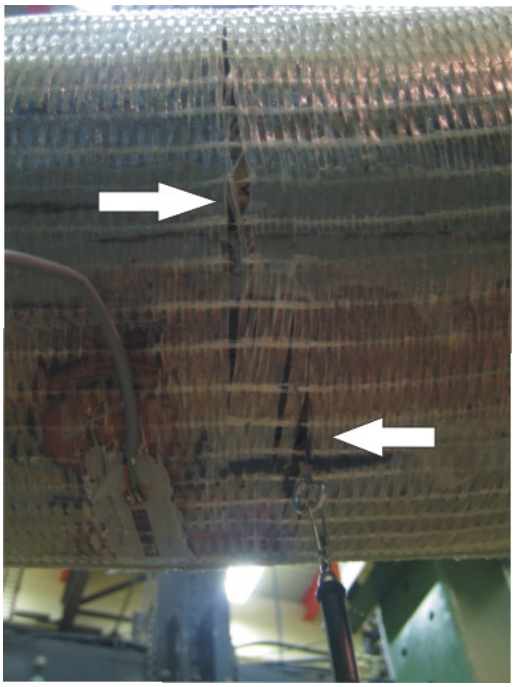

Figure 37: GFRP Splitting on the Tension Side

5.4 Strain Data Analysis

The specimens in Phases II and III of the experimental program were equipped with up to 12 strain gauges on each specimen to investigate the strain profile of the GFRP wrap. The number of configurations of the strain gauges was limited to produce consistent results that could be compared across a number of observations.

The strain gauges were installed on the GFRP wrap both around the circumference of the member and along its length. Figure 38 shows a circumferential strain gauge (Gauge 5) and a longitudinal strain gauge (Gauge 6), both installed at the mid-height of the cross section. This configuration is further explained in the following paragraphs.

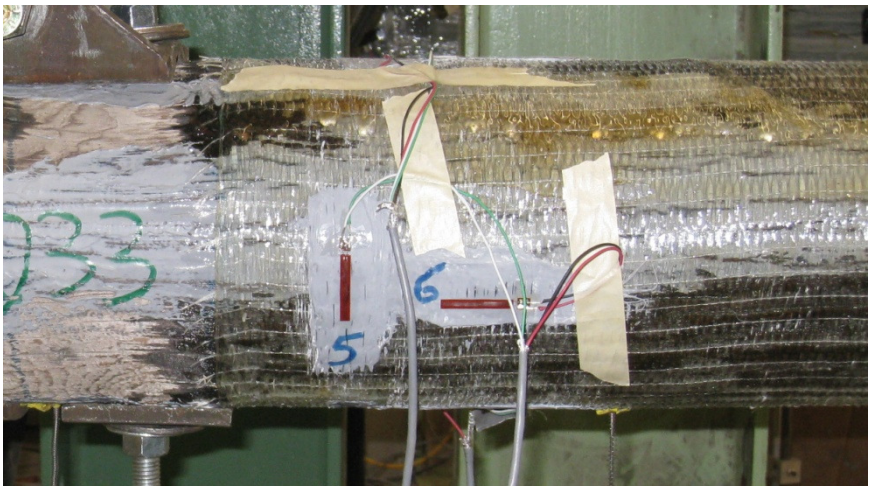

Figure 38: Circumferential and Longitudinal Strain Gauges

As explained earlier in this thesis, the purpose of the circumferential GFRP wrap was to eliminate the shear failure of the specimen and to force the failure of the strengthened cross-arms to be a pure flexure failure at the loading point. The elimination of the shear failure would result in local circumferential or hoop stresses in the GFRP wrap as shear-induced cracks and splits were confined. Analysis of the strain data indicates that since the wrap was completely bonded to the surface of the timber, the hoop strains were not uniform around the circumference of the specimen, but rather varied locally where the wood had the tendency for splitting and failing in shear. Due to the random nature of these local splits or cracks, it was not feasible to capture the maximum or peak strains at the crack locations. However, the strain data that were recorded by the strain gauges suggested a possible trend, which was confirmed by installing a large number of strategically placed strain gauges. Figure 39 shows a typical strain profile for eight strain gauges installed on the GFRP wrap around the circumference of the member at equal intervals. The strain profile shown in this figure refers to a distance of approximately 15 cm from the edge of the loading piece, towards the pinned end.

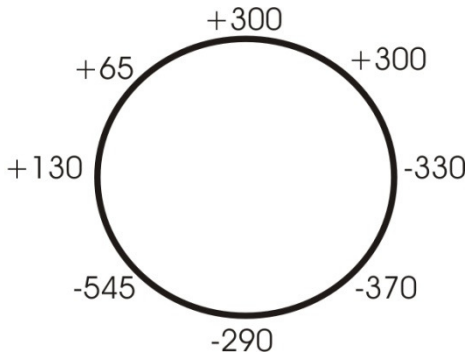

Figure 39: Typical Circumferential Strain Profile (με)

The positive strain values indicate a tension strain while the negative strain values indicate a compression strain. The values in the above figure suggested that the GFRP wrap was in circumferential compression on the bottom half of the member and in tension on the top half of it. However, in the control samples, the shear failure and splitting happened on the bottom half of the member, which would suggest that the GFRP wrap should be in tension on the bottom half of the member.

In order to address the concerns with the circumferential strain profile a number of other strain profiles were examined. One of the typical profiles is shown in Figure 40. Part A of this figure shows the circumferential strain profile, which is similar to the profile shown in Figure 39. However, in this configuration for every circumferential strain gauge, a longitudinal gauge was installed right beside it, see Figure 38. Figure 40-B shows the strain profile for the longitudinal strain gauges at the same locations shown in Part A. The purpose of testing this particular strain configuration was to test the hypothesis that the circumferential strain readings might be controlled by the Poisson's ratio effect. The consistently opposite sign of the longitudinal versus circumferential strains supported the above hypothesis.

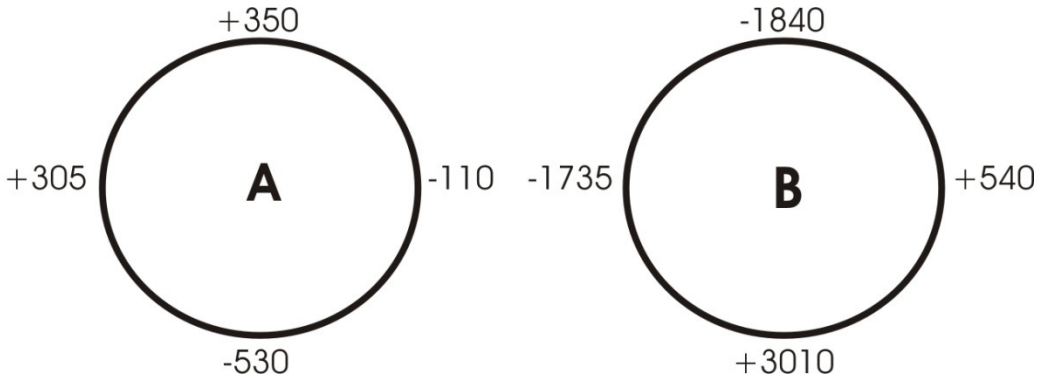

Figure 40: Typical Circumferential (A) and Longitudinal (B) Strain Profile (με)

The strain profiles shown in this Figure 40 were confirmed through a large number of repetitions. Although the values of the strains were different between different samples, the same trend and approximately the same ratio of circumferential to longitudinal strains existed in all members. Table 29 summarizes the circumferential and longitudinal strains of one specimen at different locations around the circumference of the member along with the ratio of these two strains. While the average ratio for this particular specimen was 0.19, it is important to note that the overall average ratio for all specimens approached 0.28. The overall average is a better indication of this ratio as it represents a large number of specimens. The Forest Service in United States has published a range of Poisson's Ratios for different species. For the range of pine species and for a moisture content of 14% the value of the Poisson's ratio for deformation along the radius caused by stress along the longitudinal axis was 0.335.

Since the average value obtained from the experimental program was very close to the published Poisson's Ratio, it was concluded that the strain readings around the circumference of the member were dominated by the effect of the longitudinal strains in the member. Also, the local strains due to cracks of the timber only generated some noise within the data and were not significant in any of the readings. It is also important to note that the ultimate strain of the GFRP wrap in the main direction of the fibres is 2.45%, while the maximum strain

recorded in that direction was only 0.2%. Therefore, the one layer of GFRP wrap was sufficient for the proposed strengthening system.

Table 29: Strain Ratio (Circumferential to Longitudinal)

Location	Circumferential	Longitudinal	Ratio
Top	350	-1840	0.19
Left	305	-1735	0.18
Bottom	-530	3010	0.18
Right	-110	540	0.20
Average			0.19

6 Conclusions and Recommendations

6.1 Conclusions

The main objectives of this thesis were to develop and optimize an in-situ strengthening system for the Gulfport cross-arms using Glass Fibre Reinforced Polymer (GFRP) wrap. The following conclusions are made based on the detailed analysis of the results of the three phases of the experimental program of this research.

6.1.1 Experimental Program Analysis

Phase I of the experimental program was designed to analyze the feasibility of the proposed strengthening system on Gulfport cross-arms. A total of three control specimens and three strengthened samples were tested in Phase I of the experimental program. It was concluded that the average strength of the strengthened samples was 42% higher than the strength of the control samples. The strengthened samples also demonstrated more consistent failures, while the control specimens demonstrated significantly larger scatter in the data. Phase I concluded that the proposed strengthening system was effective and that the 42% increase in capacity raised the strength of the poles beyond what was required as the design capacity of the cross arms.

The main objective of Phase II of the experimental program was to optimize the parameter configurations involved in the proposed strengthening system. Taguchi methods and Analysis of Variation (ANOVA) concepts were employed to design a statistically accurate and efficient testing program. An orthogonal array (OA8) was used for the experimental design of Phase II. The effect of four factors and two interactions were studied in this phase. Using ANOVA techniques for analysing the results of the experiments, it was concluded that the application of the filler material, non-sanded surface, and shorter width of wrap (width of 0.6 m) was the optimal parameter configuration for the proposed strengthening system. It

was also concluded that the interactions between these factors were not statistically significant. The mean of the population of the strengthened specimens, given the proposed optimal configuration, was estimated using ANOVA concepts to be approximately 128 kN. The following confidence interval was obtained for the true mean of the population of the strengthened specimens based on 95% confidence level: 115 kN < True Mean < 141 kN. The ANOVA analysis was also conducted based on the maximum bending stress as the response variable to take into account the differences in the diameters of the specimens. The 95% confidence interval, based on maximum stresses, was: 38.7 MPa < True Mean < 65.31 MPa, with a mean of 52.0 MPa.

Phase III of the experimental program of this research aimed at confirming the results and the confidence interval that were obtained using ANOVA analysis and Taguchi methods in Phase II. A total of three strengthened samples were prepared using the optimal configuration obtained in Phase II. The specimens in Phase III failed at stresses ranging from 59.6 MPa to 64.9 MPa. Therefore, not only were the samples within the originally estimated confidence interval for stresses, the results suggest that this interval could be reduced by testing more specimens. The results of Phase III of the experimental program demonstrated that despite the natural variations and uncertainties in deteriorated timber structures, the Taguchi method and ANOVA analysis could be used to obtain a more efficient experimental design in addition to providing valuable tools such as estimation of the mean and the confidence intervals.

6.1.2 Failure Modes

The control specimens failed by the combined shear-flexural failure mode. Horizontal shear cracks were formed under the loading point, in the tension region of the specimen, thus reducing the available cross section of the sample at the loading point, which then generated the flexural failure at the loading point. The application of the GFRP wrap prevented the shear failure and therefore the specimen was forced to fail in pure flexural under the loading point. Therefore, the failure of the strengthened specimens was controlled by the strength of

the wood at the point of failure. The consistency in failure modes resulted in more consistent maximum loads and stresses for the strengthened specimens in comparison to the control specimens.

Through detailed analysis of the strain data that were collected during all three phases of the experimental program, it was concluded that the strains and stresses in the GFRP wrap in the main direction of the wrap were at most only a fraction of the capacity of GFRP and thus one layer of wrap was sufficient for this application. The hoop stresses due to confinement were concluded to be present locally at random spots and on the tension side of the specimen. The corresponding strains were dominated by strains produced in the circumference of the member due to the strains in the longitudinal axis of the member, also known as Poison's effect.

6.1.3 Overall Conclusion

Based on the findings of this research program and the experimental results of all three phases, it was concluded that the strengthened specimens had much more consistent failure loads and all failed by the same failure mode. The average strength of the strengthened specimens using the optimal configuration was 70% higher than the end of life (EOL) threshold for the Gulfport cross arms. On the other hand, the failure mode of the control samples was not consistent and the failure loads were highly variable. Also, the strength values of all control samples were at or near the EOL threshold, which meant that they were no longer adequate and had to be replaced.

6.2 Recommendations

From the experimental program of this research and the related published literature on this topic, a number of recommendations are presented for improving the proposed strengthening system for Gulfport cross arms using GFRP wrap:

- Prior to the implementation of the proposed strengthening system on in-service Gulfport structures, it is highly recommended that full scale testing of the cross arms be performed in a laboratory setting. The proposed strengthening system has eliminated the most common failure mode of the Gulfport cross arms, however, the failure mode may be transferred to another location or another type and the sample may fail at loads lower than those estimated in this research project.

- Using Unidirectional Glass Fibre Reinforced Polymer wrap proved to be very efficient in increasing the strength of deteriorated circular Gulfport cross arm members. However, the proposed system did not provide any strengthening for the flexural capacity of the specimens. The use of Bidirectional GFRP wrap could improve this strengthening system as some flexural capacity would be added. Potential options for the bidirectional wrap to overpass the loading hardware and thus providing flexure reinforcement at the maximum moment point should be analyzed.

- The use of a prefabricated GFRP strip should be investigated. This prefabricated strip would be installed on the tension side of the beam, prior to the application of the confinement GFRP wrap. The prefabricated piece could be designed so that it accommodates the loading piece hardware by having varying thickness and couple of pre-drilled holes, which would allow the strip to be easily slid into place. This system would provide exceptional flexural reinforcement for the strengthened specimens.

- Special coatings should be applied to the strengthening system, after the epoxy has cured, to prevent the deterioration of the GFRP material due to sun and UV exposure.

- Lastly, the experimental results of Phase II of the experimental program suggested that the shorter width of the GFRP wrap performed better than the longer width, for the reasons discussed earlier. The use of the shorter width of wrap would cut the cost of the material by 50% and make the application process much easier. It is recommended that the use of an even shorter width of wrap be investigated to further optimize the material use and the cost of the proposed strengthening system.

Bibliography

ACI Committee 440. 2007. 440R-07 Report on Fiber-Reinforced Polymer (FRP) Reinforcement for Concrete Structures. American Concrete Institute.

Ahmed, M.R. and Lyons, J.S. 2005. Factors Affecting the Bond Between Polymer Composites and Wood. *Journal of Reinforced Plastics and composites,* 24(4), 405-412

Alampalli, S. 2001. Fibre Reinforced Polymers for Rehabilitation of Bridge Columns. *Fifth National Workshop on Bridge Research in Progress,* Minneapolis, Minnesota, 37-42.

American Society of Testing and Materials (ASTM). Committee D-7 on Wood. Phadelphia, PA. 2007

- D143-94 Standard Test Methods for Small Clear Specimens of Timber

Au, C. and Buyukozturk, O. 2005. Effect of Fibre Orientation and Ply Mix on Fibre Reinforced Polymer Confined Concrete. *Journal of Composites for Construction,* 9(5), 397-407

Barker, T.B. 1990. Engineering Quality by Design: Interpreting the Taguchi Approach. ASQC Quality Press, Milwaukee, Wisconsin.

Batish, A. 2007. ME747: Experimental Design and Taguchi Methods. Course Notes, University of Waterloo, Waterloo, ON, Canada.

Belavendram, N. 1995. Quality by Design: Taguchi Techniques for Industrial Experimentations. Prentice Hall, Hertfordshire, UK.

Bendell, A., Disney, J., and Pridmore, W.A. 1989. Taguchi Methods: Applications in World Industry. IFS Publications, UK.

Bonacci, J.F., Hearn, N., Pantazopoulou, S.J., Sheikh, S., and Thomas, M.D.A. 2001. Repair of Corrosion-Damaged Columns with FRP Wraps. *Journal of Composites for Construction.* 5(1), 3-11

Borri, A., Corradi, M., Grazini, A. 2005. A method for flexural reinforcement of old wood beams with CFRP materials. *Journal of Composites Parts B: Engineering.* 36(2), 143-153

Canadian Standard Association (CSA). 1990. CAN/CSA – O15-90, Wood Utility Poles and Reinforcing Stubs, Toronto, Ontario

Canadian Standards Association (CSA). 2001. CSA C22.3 No. 1-01, Overhead Systems, Toronto, Ontario

Chahrour. A.H. and Soudki, K.A. 2006. Structural Retrofitting of Deteriorated Concrete Lighting Poles Using FRP Sheets in Wet Layup-Field Application. *Journal of Composites for Construction,* 10(3), 234-243.

Davalos, J.F., Qiao, P., and Zipfel, M.G. 1999. Feasibility Study of Prototype GFRP-Reinforced Wood Railroad Crosstie. *Journal of Composites for Construction.* 3(2), 92-99

Dehnad, K. 1988 Quality Control, Robust Design, and The Taguchi Method. Arcata Graphics, Fairfield, Pennsylvania.

Gentile, C., Svecova, D., and Rizkalla, S.H. 2002. Timber Beams Strengthened with GFRP Bars: Development and Application. *Journal of Composites for Construction,* 6(1), 11-20

Gilbert, S.G., Gilfillan, J.R., and Patrick, G.R.H. 2003. The Use of FRP Composites in Enhancing the Structural Behaviour of Timber Beams. *Journal of Reinforced Plastics and Composites,* 22(15), 1373-1388

Ho, V.W.K. 2005. Strength Assessment of Wood Cross arms Using Image Processing Techniques. MASc Thesis, University of Waterloo, Waterloo, ON, Canada .

McCarthy, F.J. 2005. Condition Assessment of Wooden Cross arms in 230 KV Transmission Structures. MASc. Thesis, University of Waterloo, Waterloo, ON, Canada.

Mirmiran, A. and Shahawy, M. 1997. Behaviour of Concrete Columns Confined by Fibre Composites. *Journal of Structural Engineering,* 123(5), 583-590

Nanni, A. and Norris, M.S. 1995. FRP Jacketed Concrete under Flexure and Combined Flexure-Compression. *Journal of Construction and Building Materials,* 9(5), 273-282

Natural Resources Canada and U.S. Department of Energy. 2003. Interim Report: Causes of the August 14th Blackout in the United States and Canada. U.S.-Canada Power System Outage Task Force, Toronto, Ontario

Roy, R.K. 2001. Design of Experiments Using the Taguchi Approach: 16 Steps to product and process improvement. John Wiley & Sons Inc, New York, New York.

Shahi, A., West J.S., and Pandey M.D. 2008. “Parametric Optimization of The Strengthening of Gulfport 230 kV Transmission Structures with Glass Fibre Reinforced Polymer (GFRP) Wrap”, 5th International Conference on Advanced Composite Materials in Bridges and Structures (ACMBS-V), Winnipeg, Manitoba, Canada, Sept. 22-24

Shahi, A., West, J.S., and Pandey, M.D. 2007. “Strengthening of 230kV Wood Transmission Structures with Glass Fibre Reinforced Polymer (GFRP) Wraps”, CSCE 2007 Annual General Conference, Yellowknife, Northwest Territories, Canada, June 6-9.

U.S. Department of Agriculture. General Technical Report FPL-GTR-113. *Wood Handbook – Wood as an Engineering Material.* Forest Products Laboratory, Madison, WI. 1999.

Wood Design Manual (2005). Canadian Wood Council. Friesens, Altona, MB.

Wynn, H.P. and Logothetis, N. 1989. Quality Through Design: Experimental Design, Off-line Quality Control, and Taguchi’s Contributions, Oxford, New York.